A Middle Path for On-Premises LLM Deployment: Preserving Privacy Without Sacrificing Model Confidentiality

Hanbo Huang[1], Yihan Li[2], Bowen Jiang[1], Bo Jiang[1], Lin Liu[2], Ruoyu Sun[3], Zhuotao Liu[4], Shiyu Liang[1]
[1]Shanghai Jiao Tong University, [2]National University of Defense Technology,
[3]Chinese University of Hong Kong (Shenzhen), [4]Tsinghua University
{hhuang417,lsy18602808513}@sjtu.edu.cn

Abstract

Privacy-sensitive users require deploying large language models (LLMs) within their own infrastructure (*on-premises*) to safeguard private data and enable customization. However, vulnerabilities in local environments can lead to unauthorized access and potential model theft. To address this, prior research on small models has explored securing only the output layer within hardware-secured devices to balance model confidentiality and customization. Yet this approach fails to protect LLMs effectively. In this paper, we discover that (1) query-based distillation attacks targeting the secured top layer can produce a functionally equivalent replica of the victim model; (2) securing the same number of layers, bottom layers before a transition layer provide stronger protection against distillation attacks than top layers, with comparable effects on customization performance; and (3) the number of secured layers creates a trade-off between protection and customization flexibility. Based on these insights, we propose SOLID, a novel deployment framework that secures a few bottom layers in a secure environment and introduces an efficient metric to optimize the trade-off by determining the ideal number of hidden layers. Extensive experiments on five models (1.3B to 70B parameters) demonstrate that SOLID outperforms baselines, achieving a better balance between protection and downstream customization. Our code can be found at: https://github.com/OTTO-OTO/SOLID-OnPremiseDeployment.

1 Introduction

Vendors of Large Language Models (LLMs) have introduced advanced models with remarkable capabilities to address diverse user needs (Minaee et al., 2024; Zhao et al., 2023). To meet specific customization demands, vendors typically adopt two approaches. Closed-source vendors, such as OpenAI, provide fine-tuning APIs that allow users to upload data to customize proprietary models like GPT-4. In contrast, vendors like Meta offer open-weight models such as Llama3 (Dubey et al., 2024), which users can adapt within their own infrastructure, ensuring greater flexibility and control.

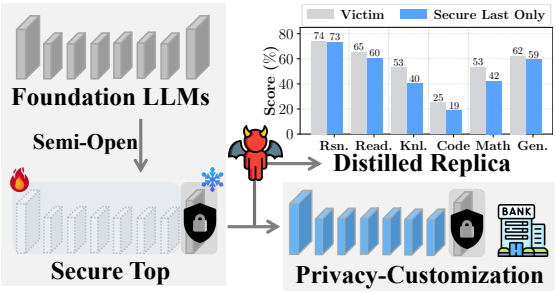

Figure 1: Semi-open Deployment.

However, both approaches present notable limitations for privacy-sensitive users, such as healthcare organizations, who prioritize data security. Strict regulations prohibit these users from uploading sensitive data to third-party API services, necessitating *on-premises deployment* of LLMs, where data processing and model customization are confined to local infrastructure (Nevo et al., 2024). Although fine-tuning open-weight models in such environments offers a viable path for customization, full disclosure of model architectures and weights increases the risk of exploitation by malicious actors, who may circumvent safety mechanisms (Hendrycks et al., 2023). Consequently, vendors may be hesitant to release SOTA models as open-weight, since uncontrolled access could lead to significant harm. Moreover, maintaining high-quality open-weight models imposes considerable computational and financial burdens (Wolfe et al., 2024). These growing concerns highlight the importance of *secure on-premises deployment of closed-source models*, which preserves control and ensures regulatory compliance.

Despite the advantages, deploying closed-source LLMs locally introduces the risk of model theft. Unauthorized users can extract model parameters and architectures directly from CPUs and memory

Proceedings of the 2025 Conference on Empirical Methods in Natural Language Processing, pages 8333–8371
November 4-9, 2025

within local environments (Hu et al., 2020). To mitigate this, existing approaches use Trusted Execution Environments (TEEs) to protect proprietary models (Nayan et al., 2024; Narra et al., 2019). Yet, fully enclosing large models within TEEs results in prohibitive computational overhead, limiting their practicality (Li et al., 2024a).

Prior research has explored to mitigate this trade-off by securing only critical layers, such as the output layer, while leaving the remaining layers exposed for fine-tuning (Zhang et al., 2024b; Mo et al., 2020). However, studies have shown that even with only black-box access, adversaries may still be able to replicate the weights of DNNs (Tramèr et al., 2016; Truong et al., 2021). More recent works (Carlini et al., 2024; Finlayson et al., 2024) further suggests that the final-layer weights of large language models (LLMs) can be recovered from output logits alone, raising concerns about the robustness of such partial protection strategies. Consistent with previous findings, our results show that this partial protection remains vulnerable to distillation attacks (Zanella-Beguelin et al., 2021). When extended to Llama2-70B, we confirm that attackers can still extract nearly complete model functionality across six domains, as illustrated in Figure 1. These vulnerabilities raise skepticism about *whether model confidentiality and customization can truly coexist in on-premises deployment*, highlighting the need for security paradigms beyond output-layer protection.

In this paper, we show that this dilemma can be resolved. We begin by investigating the security-customization trade-off introduced by the placement of secured layers in LLMs. Specifically, we theoretically identify a transition layer in deep transformers, showing that securing bottom layers before this transition significantly reduces distillation success, while securing top layers has a more limited impact. Besides, we demonstrate that the number of secured layers creates a trade-off: securing more layers improves security but reduces customization flexibility. To optimize this trade-off, we introduce SOLID, a semi-open deployment framework that selectively secures a subset of bottom layers, using a distillation difficulty score to identify the optimal set for protection. Our experiments show that SOLID balances security and customization, achieving security comparable to fully secured models while maintaining strong customization flexibility, approaching full parameter fine-tuning. Our main contributions are as follows:

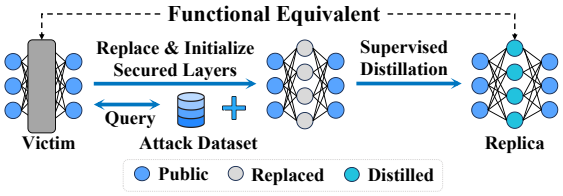

Figure 2: Workflow of model distillation attack

- We extend query-based distillation attacks to LLMs, demonstrating that existing on-premises frameworks risk full functionality replication.
- We identify the security-customization trade-off introduced by the placement of secured layers, and theoretically prove that securing bottom layers before the transition layer offers stronger protection with similar customization effects.
- We discover that the number of secured layers affects both security and customization. We propose SOLID, which optimizes the security-customization trade-off by using a fine-tuning-free metric to secure minimal bottom decoder layers, protecting the model from distillation attacks while preserving customization flexibility.
- We evaluate SOLID against three baselines across five models (1.3B to 70B parameters), assessing security across three distillation strategies on sixteen benchmarks and customization flexibility across six tasks. Extensive experiments show SOLID effectively balances security and customization, despite some limitations

2 Preliminaries

2.1 Security Threat: Model Distillation

Adversary's Objective. The adversary aims to replicate the functionality of a semi-open victim LLM, partially secured in a protected environment, by training a substitute model. This replica facilitates white-box analysis to identify vulnerabilities, enhancing black-box attacks on related model families (Sitawarin et al., 2024). The agreement between the victim and replica is assessed via accuracy and fidelity on a designated test set.

Adversary's Knowledge. It is assumed that the adversary knows the architectures of both secured and unsecured modules, as prior work (Gou et al., 2021; Boix-Adsera, 2024) has shown that using the same architecture as the secured module significantly improves the effectiveness of distillation attacks. However, the adversary knows only the parameters of the unsecured module, while those of the secured module remain unknown.

Adversary's Capability. The adversary is capable of querying the semi-open model, obtaining both the semantic output produced by the complete model and the representation vector generated by the secured module. Utilizing this information, the adversary constructs a distillation attack dataset denoted as $\mathcal{D}$. Since the adversary knows the architecture of the secured module, the adversary next replaces the secured module with a randomly initialized module of the same architecture. Using the constructed set $\mathcal{D}$, the adversary employs three distinct supervised distillation strategies to replicate the functionality of the secured module: (1) **FT-all:** Fine-tunes both the replacement and unsecured modules using output of the entire model as training labels. (2) **FT-closed:** Fine-tunes only the replacement model using output of the entire model, keeping the unsecured module fixed. (3) **SEM** (Tamber et al., 2024): Fine-tunes the replacement model using outputs from the secured module without involving the unsecured component.

2.2 Problem Formulation

In this paper, we analyze the performance of a large language model under a defined distribution $\mathbb{P}_{\mathbf{X}\times Y}$, describing the relationship between input matrix $\mathbf{X}$ and label Y. We assume the victim LLM $f(\mathbf{X};\boldsymbol{\theta})$ performs well on this distribution, and the attack set $\mathcal{D}$ comprises samples drawn from $\mathbb{P}_{\mathbf{X}\times Y}$. To evaluate agreement between the distilled LLM and ground-truth labels, we use a scoring function $s : \mathcal{Y} \times \mathcal{Y} \to \mathbb{R}^+$. Secured layers are indexed by $I \subseteq [L] = \{1, \ldots, L\}$. Let $\boldsymbol{\theta}_{\text{dist}}(I, \mathcal{D})$ represent the parameter vector of the distilled replica of a victim model, where layers indexed by I are secured, and adversaries utilize the attack set $\mathcal{D}$ to replicate its functionality. For each secured set I, we define the "**Distillation Ratio**" $R(I)$, which quantifies how well the distilled model $\boldsymbol{\theta}_{\text{dist}}(I, \mathcal{D})$ replicates the behavior of $f(\mathbf{X};\boldsymbol{\theta})$, expressed as

$$R(I) = \frac{\mathbb{E}[s(f(\mathbf{X};\boldsymbol{\theta}_{\text{dist}}(I,\mathcal{D})), Y)]}{\mathbb{E}[s(f(\mathbf{X};\boldsymbol{\theta}), Y)]}. \quad (1)$$

Here, $\mathbb{E}$ in the numerator reflects the expectation computed over random samples $(\mathbf{X}, Y)$ drawn from $\mathbb{P}_{\mathbf{X}\times Y}$, the random attack set $\mathcal{D}$, and the random initialization of parameters within the secured layers during fine-tuning. Conversely, the term $\mathbb{E}$ in the denominator solely considers the expectation over random samples. With this definition, $R([L])$ represents the distillation ratio when the entire model is secured, reflecting the highest level of security. This leads to the question:

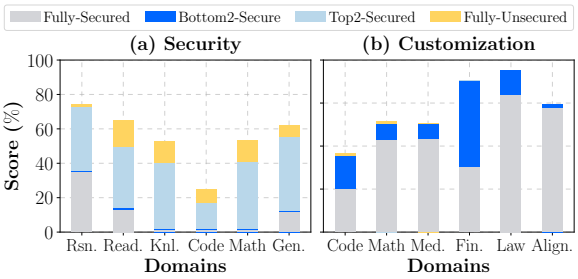

Figure 3: Security and adaptability comparison in Llama2-70B. Lower scores indicate better security in Fig. (a) and weaker adaptability in Fig. (b). Details can be found in Appendix C.1

What is the smallest secured set I such that $R(I)$ closely approximates $R([L])$?

This question aims to identify the minimal secured set I such that securing the layers indexed by I achieves a level of security comparable to securing the entire model.

3 Methodology

In this section, we investigate the impact of securing specific layers on security and customization against distillation attacks. We begin with an experiment with two semi-open deployments of Llama2-70B: one securing the bottom two decoder layers (Bottom2-Secured) and the other securing the top two decoder layers (Top2-Secured). As shown in Figure 3, both deployments achieve similar customization performance in six downstream tasks. However, securing the bottom layers provides significantly stronger security. Additionally, comparing Bottom2-Secured to fully-secured deployment reveals comparable security with improved customizability. This suggests that securing a certain number of bottom layers can effectively balance strong security against distillation attacks and high customization performance.

3.1 Security Transition in Deep Transformers

Model Overview. In this subsection, we consider a deep transformer f with L layers, expressed as $f(\mathbf{X};\boldsymbol{\theta}) = \varphi_L \circ \cdots \circ \varphi_1(\mathbf{X})$. The input feature matrix $\mathbf{X} \in \mathbb{R}^{n\times d}$ consists of n rows, each representing a d-dimensional token vector. Each layer φ_i is a transformer that incorporates a normalized residual self-attention mechanism, defined as:

$$\varphi_i(\mathbf{X}; K_i, Q_i) = \mathbf{X} + \text{softmax}\left(\frac{\mathbf{X}Q_i(\mathbf{X}K_i)^\top}{\sqrt{d_Q}\,\|\mathbf{X}\|^2}\right)\mathbf{X}$$

Here, $Q_i \in \mathbb{R}^{d\times d_Q}$ and $K_i \in \mathbb{R}^{d\times d_Q}$ are projection matrices for the query and key components, respectively. The terms $\sqrt{d_Q}$ and $\|\mathbf{X}\|$ serve as normalization factors, ensuring stable computations within the attention mechanism. We consider the semi-open deployment of securing the αL-th layer with $\alpha \in [0,1]$ and $\alpha L \in \mathbb{N}$ while keeping other layers unsecured. After the distillation attack, we assume the parameters of the distilled model in the unsecured layers are identical to the victim model, while those in the secured layer deviate. Let $\hat{K}_{\alpha L}$ and $\hat{Q}_{\alpha L}$ denote the distilled weight matrix of the proprietary layer, i.e., $\boldsymbol{\theta}_{\text{dist}}(\{\alpha L\}) = \{(K_1,Q_1),...,(\hat{K}_{\alpha L},\hat{Q}_{\alpha L}),...,(K_L,Q_L)\}$. Let $\hat{\varphi}_{\alpha L}$ denote the function of the distilled proprietary layer, i.e., the $\alpha L-$th layer, in the distilled model. In this subsection, we consider the normalized output of an infinitely deep model whose αL-th layer is hidden and subjected to the attack. The output of the distilled model is

$$\hat{f}_\infty(\mathbf{X}) = \lim_{L\to\infty} \frac{f(\mathbf{X};\boldsymbol{\theta}_{\text{dist}}(\{\alpha L\}))}{\|f(\mathbf{X};\boldsymbol{\theta}_{\text{dist}}(\{\alpha L\}))\|_F},$$

where $\|\cdot\|_F$ denotes the Frobenius norm. We consider an infinitely deep network as the ideal model, reflecting the sufficient depth of most large-scale models in practice. The following theorem establishes the existence of a critical value α^* such that if $\alpha < \alpha^*$, the output matrix of the distilled LLM has rank one. Conversely, if $\alpha > \alpha^*$, the output matrix has rank strictly greater than one.

Theorem 1. *Assume that $\mathbb{P}_{\mathbf{X}\times Y}$ is defined on a countable domain $\mathcal{X}\times\mathcal{Y}$ with $\mathbf{0}_{n\times d} \notin \mathcal{X}$. Assume that parameter matrices $\{K_i,Q_i\}_{i\geq 1}$ in the victim model f have uniform bounded norms, i.e., $\|K_i\| \leq D$ and $\|Q_i\| \leq D$ for some $D > 0$. There exists an $\alpha^* \in (0,1)$ depending on D such that the following two statements are true.*

(1) If $\alpha < \alpha^*$ and $\{K_i,Q_i\}_{i\geq 1}$ are parameter matrices of the victim model, with $\hat{K}_{\alpha L}$ and $\hat{Q}_{\alpha L}$ as distilled parameters drawn from a continuous distribution on $\mathbb{R}^{n\times d}$, the matrix $\hat{f}_\infty(\mathbf{X})$ almost surely has rank one for all inputs $\mathbf{X}$.

(2) If $\alpha > \alpha^*$, there exists a victim model with parameter sequence $\{K_i,Q_i\}_{i\geq 1}$ such that for any distilled parameters $\hat{K}_{\alpha L}$ and $\hat{Q}_{\alpha L}$, the matrix $\hat{f}_\infty(\mathbf{X})$ has rank greater than one for some $\mathbf{X}$.

Remark 1: The proof is provided in Appendix A. This theorem demonstrates that if the distilled parameters of the bottom layers (i.e., $\alpha < \alpha^*$) are obtained through a randomized algorithm, such as stochastic gradient descent, with a continuous distribution supported on $\mathbb{R}^{n\times d}$, the distillation will certainly fail, as the feature matrix degenerate. In contrast, keeping the later layers secured (i.e., $\alpha > \alpha^*$) does not maintain this property, indicating that it is more effective to secure the bottom layers before the transition layer, rather than the later ones. Further remarks are in Appendix A.5.

3.2 SOLID: Semi-Open Local Infrastructure Deployment Framework

Theorem 1 shows that securing bottom layers improves security. Inspired by this insight, we propose a method to approximately find the smallest bottom layer index set I that satisfies $R(I) \leq (1+\varepsilon)R([L])$ for any small $\varepsilon > 0$. To achieve this, a straightforward implementation is to begin with A simple approach is to start with $I_l = \{1,\ldots,l\}$ for each l beginning from 1, then evaluate the distillation ratio $R(I_l)$ after the attack, and identify the smallest l that meets the inequality. This extensive fine-tuning process is time-consuming, prompting the critical question: *Can we create a fine-tuning-free metric that predicts LLM performance under model distillation attacks?* Hence, our goal is to establish a metric directly correlated with the distillation ratio.

In the distillation ratio $R(I)$, each I has the same denominator, so our focus is on a metric related to the numerator, specifically $\mathbb{E}[s(f(\mathbf{X};\boldsymbol{\theta}_{\text{FT}}(I,\mathcal{D})),Y)]$, which measures the average performance score of the distilled model. This average performance score generally inversely correlates with the average testing loss with the expression $L(\boldsymbol{\theta}) \triangleq \mathbb{E}_{\mathbf{X}\times Y}[\ell(f(\mathbf{X};\boldsymbol{\theta}),Y)]$, where ℓ denotes the cross-entropy loss employed by LLM. Hence, we aim at finding the smallest I such that

$$L(\boldsymbol{\theta}_{\text{dist}}(I,\mathcal{D})) \geq (1-\varepsilon)L(\boldsymbol{\theta}_{\text{dist}}([L],\mathcal{D})).$$

However, calculating both sides of this inequality requires knowing the distilled parameters from the fine-tuning process. To bypass this, we aim for an approximate solution. The distilled parameters are generated through gradient descent, starting from the initial parameters $\boldsymbol{\theta}_0(I)$, with the hidden layers being randomly initialized. Using the Taylor Expansion, we find

$$L(\boldsymbol{\theta}_{\text{dist}}(I,\mathcal{D})) = L(\boldsymbol{\theta}_0(I,\mathcal{D})) + \mathcal{O}(\mathbb{E}\|\boldsymbol{\theta}_{\text{dist}}(I,\mathcal{D}) - \boldsymbol{\theta}_0(I)\|_2).$$

Previous research (Choi et al., 2024; Bailly et al., 2022) indicates that the difference $\|\boldsymbol{\theta}_{\text{dist}}(I,\mathcal{D}) -$

$\boldsymbol{\theta}_0(I)\|_2$ is minimal in large networks compared to the dataset size $|\mathcal{D}|$. In models such as single-layer ReLU networks (Anthony et al., 1999; Zou et al., 2020), this difference scales as $\mathcal{O}\left(\frac{|\mathcal{D}|}{\sqrt{N}}\right)$ (Jacot et al., 2018; Wei et al., 2019), where N, the number of model parameters, far exceeds the dataset size in large language models (LLMs) (Dubey et al., 2024; Liu et al., 2024). The first term, independent of fine-tuning, dominates and effectively predicts the distillation ratio. We refer to this term as the **Distillation Difficulty** (DD(I)), defined as

$$\text{DD}(I) = \mathbb{E}[L(\boldsymbol{\theta}_0(I))].$$

This score, which can be estimated using a sample average, represents the distilled model performance of the model when specific layers I are secured. A higher **DD**(I) suggests better security performance, indicating a lower distillation ratio $R(I)$. Therefore, our SOLID operates in the following way. SOLID begins by sampling evaluation data targeting general capabilities from the underlying distribution, and then computes DD(I_l) for each set of secured layers $I_l = \{1, ..., l\}$ for $l = 1, ..., L$. SOLID stops at the smallest l^* that satisfies DD(I_{l^*}) $\geq (1 - \varepsilon)$DD($[L]$).

4 Experiments

In this section, we conduct experiments to answer the following research questions:

- **RQ1.** Can query-based distillation attack distill the functionality of the entire model under the baseline deployment that secures the top layer?
- **RQ2.** How do secured layer location and amount affect the security-customization trade-off?
- **RQ3.** Does SOLID offer a better balance between model theft risk and customization performance compared to baseline deployments?
- **RQ4.** How does SOLID optimize this trade-off? Is it effective for both large and small models?

4.1 Experimental Settings

We begin by introducing our experimental setups. Details can be found in Appendix B.

Models. We consider **five** open-source, decoder-only structured LLMs with various architectures. Specifically, we select Llama2-70B-chat, Llama2-7B-chat (Touvron et al., 2023), Mistral-7B-v0.1 (Jiang et al., 2023), Phi-2 (Abdin et al., 2024), and Phi-1.5 (Li et al., 2023). We designate these pre-trained models as the base models for adaptation and victims in model distillation attacks.

Attack Methods. We distill models produced by different protection approaches using three attack methods: FT-all, FT-closed and SEM. Following (He et al., 2021), a diverse attack set is required for full distillation. Therefore, we merge data evenly from two general datasets, MMLU benchmark (Hendrycks et al., 2021) and Alpaca 52k (Wang et al., 2022), resulting in a 51k combined set. Additionally, we build four larger general datasets (100k–500k) to strengthen the attack.

Baselines. We compare SOLID with three baselines: SAP-DP, the fully-secured approach (Eiras et al., 2024), and DarkneTZ (Mo et al., 2020). The SAP (Shen et al., 2023) framework exposes the first six decoder layers and secures the rest. SAP-DP extends SAP by adding Laplace noise to model outputs to enhance protection (Lee et al., 2018). The fully-secured approach represents the extreme, securing all layers for maximal security, while DarkneTZ protects only the final decoder layer.

Implementation Details of SOLID. We apply the SOLID algorithm to identify the smallest secure set I such that $R(I) \leq (1+\varepsilon)R([L])$. To calculate distillation difficulty (DD), we use cross-entropy loss and approximate the expectation over samples distributed on the general domain and randomly initialized secured parameters. This is done using a 1,500-sample evaluation set randomly sampled from the MMLU benchmark and Alpaca 52k, with secured parameters initialized via Xavier initialization and averaged over three random seeds (20, 42, 1234). In our experiments, we find that $\varepsilon = 0.05$ yields optimal performance.

Evaluation Benchmarks We assess adaptability on six downstream tasks: Code (Zheng et al., 2024a), Math (Yue et al., 2023), Medical (Zhang et al., 2023), Finance (Wang et al., 2023a), Law (Guha et al., 2024), and Alignment (Meng et al., 2024). To fully evaluate recovered functionalities, we focus on six capabilities domains following Llama2 report (Touvron et al., 2023). Specifically, we assess the recovered model across **sixteen** benchmarks grouped into (1) *Commonsense Reasoning* (Rsn.); (2) *Reading Comprehension* (Read.); (3) *World Knowledge* (Knl.); (4) *Code*; (5) *Math*; and (6) *General Ability* (Gen.).

Metrics. We measure customization through model's improvements on benchmarks. For security, we calculate the "Average Distillation Ratio" (ADR) by averaging the distillation ratios across benchmarks. A lower ADR indicates higher security offered by the secure set.

	Benchmark	Llama2-70B	Llama2-7B	Mistral-7B	Phi-2
Rsn.	PIQA	62.6|59.8|63.0|99.3	64.7|64.7|64.6|99.1	63.0|61.2|60.2|92.2	68.3|65.6|65.7|99.1
	Winogrande	68.5|67.7|68.3|98.3	76.8|74.8|76.6|100.	67.2|69.0|68.3|89.5	68.3|64.9|64.8|99.1
	ARC-easy	31.9|32.8|31.3|98.5	36.3|35.5|34.9|97.6	32.3|34.7|32.0|86.6	43.2|35.3|33.9|99.5
	ARC-challenge	38.5|38.1|44.2|99.2	47.8|46.6|50.9|100.	39.7|42.6|44.5|81.4	36.8|36.6|35.3|99.5
	Hellaswag	31.4|31.4|32.4|98.1	33.9|34.0|35.0|96.6	32.2|32.0|31.3|84.6	37.4|37.3|34.3|96.5
Read.	LAMBADA	0.01|0.00|0.00|88.6	0.02|0.00|0.01|92.2	0.16|0.00|0.01|67.9	1.34|0.04|0.00|94.6
	BoolQ	47.2|47.1|53.9|100.	59.5|56.0|65.0|99.6	48.3|46.8|56.7|97.3	56.7|50.3|55.8|100.
	SQuADv2	1.50|1.68|0.34|55.3	0.68|0.88|0.82|59.5	1.69|0.36|0.93|50.7	3.65|0.39|0.90|62.9
	OBQA	54.5|54.5|57.1|99.6	57.4|52.5|59.2|94.8	57.7|56.8|56.3|84.0	0.00|0.00|0.02|94.3
Knl.	NaturalQuestions	0.00|0.02|0.00|40.1	0.01|0.01|0.08|53.6	0.00|0.00|0.02|31.8	0.01|0.00|0.06|87.4
	TriviaQA	0.00|0.02|0.00|72.3	0.00|0.00|0.03|73.8	0.00|0.00|0.01|38.7	0.01|0.00|0.01|68.9
Code	MBPP&H.E.	0.00|0.00|0.00|58.6	0.00|0.00|0.00|90.9	0.00|0.00|0.00|40.2	0.00|0.00|0.00|91.1
Math	GSM8K	0.02|0.00|0.06|79.6	0.00|0.00|0.00|78.6	0.00|0.00|0.00|31.1	0.00|0.00|0.00|86.2
Gen.	MMLU	36.8|38.3|36.5|96.7	52.9|50.0|53.3|110.	40.4|36.9|37.2|81.7	42.6|40.3|40.5|99.5
	BBH	0.00|0.00|0.00|93.3	0.00|0.00|0.00|101.	0.00|0.00|0.00|63.3	0.01|0.00|0.00|94.8
Average Distillation Ratio(↓)		**21.9**|21.8|22.8|**77.9**	**25.3**|24.4|25.9|**86.5**	**22.5**|22.4|22.8|**73.7**	**23.9**|22.3|22.4|**88.9**
Secured Ratio(↓)		**2.50**|92.5|100.|**1.25**	**3.16**|81.3|100.|**3.16**	**3.16**|81.3|100.|**3.16**	**6.25**|81.3|100.|**3.16**

Table 1: Distillation ratios across six functionalities under FT-all (SOLID|SAP-DP|Fully-secured|DarkneTZ). "H.E." in the Code domain denotes the benchmark HumanEval. Green and red indicate the overall best- and worst-performing methods, respectively. Additional results are provided in Appendix C.2.

4.2 Failure in Defense (RQ1)

We evaluate security of DarkneTZ using three distillation strategies. Based on the results shown in Tables 1 and 2, we have following observations.

Obs1: DarkneTZ, which secures only the last decoder layer, fails to protect the model against all three attacks. As shown in Table 1, DarkneTZ achieves ADRs generally exceeding 73%. Notably, on Llama2-7B, it surpasses 100% distillation ratio on the MMLU and BBH datasets, indicating that the distilled model outperforms the original on these tasks. Similarly, Table 2 highlights consistent failure patterns against FT-closed and SEM attacks, with DarkneTZ maintaining ADRs above 75%, demonstrating the ability of these strategies to recover significant model functionality.

4.3 Security-Customization Trade-off (RQ2)

We conduct two experiments to analyze the impact of secured layer placement and quantity on the trade-off between security and customization. First, we secure one layer in Llama2-7B and two in Phi-2, varying their placement. Second, we incrementally secure both models by adding protected layers, starting from the smallest module (`k_project`) of the first decoder layer. These models are evaluated under the FT-all distillation attack and customized for the math domain. The results, as shown in

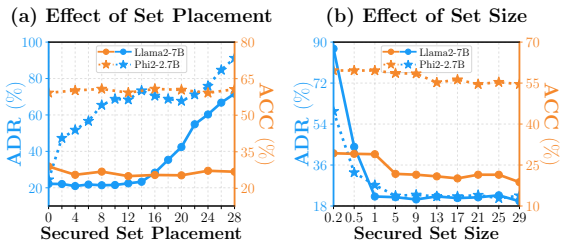

Figure 4: (a) shows the trade-off between security and customization for Llama2-7B and Phi-2 with different placements of same-sized secured sets. (b) shows the trade-off as the secured set size increases from the first decoder layer. Smaller ADR indicates higher security and higher ACC reflects better customizability.

Figure 4, lead to the following observations.

Obs2: Secured layer placement significantly impacts security, consistent with Theorem 1, but has small effect on customization performance. As shown in Figure 4(a), for Llama2-7B, security transitions at the fourteenth layer, with ADR consistently near 20% for earlier sets, indicating stronger security than protecting later layers. Meanwhile, customization accuracy remains stable across placements, highlighting the advantage of securing pre-transition layers. In contrast, Phi-2 transitions earlier at the first layer set, where only the first set balances security and customization, with later sets reducing security. These results suggest that securing layers before the transition layer optimizes the security-customization trade-off. Results for

Strat.	Method	Rsn.	Read.	Knl.	C.&M.	Gen.	ADR
FT-c.	SOLID	47.1	21.6	0.00	0.03	18.7	22.6
	SAP-DP	46.2	19.5	0.00	0.00	19.0	21.8
	F-Secured	47.8	21.2	0.00	0.08	18.5	22.8
	DarkneTZ	98.7	69.3	58.3	65.9	95.0	78.1
SEM	SOLID	48.2	21.9	0.00	0.00	18.5	22.4
	SAP-DP	47.1	21.1	0.00	0.00	18.3	22.3
	F-Secured	47.8	21.2	0.00	0.08	18.5	22.8
	DarkneTZ	98.8	71.2	54.2	66.3	94.1	77.4

Table 2: Distillation ratios of Llama2-70B under FT-closed and SEM attacks.

Mistral-7B and Phi-1.5 are in Appendix B.7.

Obs3: Increasing the number of secured layers enhances security but reduces customization. As shown in Figure 4(b), the ADR of Llama2-7B decreases from 85% to 22% after securing an entire decoder layer, indicating improved security. However, customization accuracy drops from 29% to 21% as the number of secured layers increases from one to five, reflecting reduced customization flexibility. A similar trend is observed in Phi-2, suggesting that while increasing the number of secured layers enhances security (lower ADR), it negatively impacts customization flexibility (lower ACC) in both models. Further details are in Appendix B.8.

4.4 Effectiveness of SOLID (RQ3)

We compare the security of SOLID with baseline deployments across three distillation strategies. The results lead to the following observations.

Obs4: SOLID offers comparable security against model distillation to the highest level of protection (fully-secured), while securing significantly fewer parameters. As shown in Table 1, SOLID achieves a similar security level (ADR) to SAP-DP and the fully-secured approach across four architectures and various domains, while securing at most 6.25% of parameters, compared to at least 80% for the others. For example, on Llama2-70B, SOLID secures only 1.25% of parameters yet achieves an ADR of 21.9%, comparable to SAP-DP (21.8%) and the fully-secured approach (22.8%), which protect 92.5% and 100% of parameters, respectively. Furthermore, under FT-closed and SEM attacks, SOLID also matches the security level provided by SAP-DP and the fully-secured approach. Table 2 shows that under FT-closed attack, the ADR differences between SOLID, SAP-DP, and the fully-secured approach remain below 2.1% across six domains. Similarly, under SEM attack, the distillation ratios closely aligned with the other two approaches. These results confirm that SOLID effectively protects against distillation attacks while securing significantly fewer parameters. More details are in Appendix C.4 and C.5.

Scale	Rsn.	Read.	Knl.	C.&M.	Gen.	ADR	ADR-Da.
51k	51.7	21.6	0.01	0.00	28.3	25.3	86.5
100k	51.3	21.5	0.13	0.00	29.6	25.3	89.1
200k	51.4	21.7	0.11	0.00	29.7	25.2	91.3
300k	51.6	21.7	0.11	0.00	30.5	25.5	94.5
500k	51.8	22.0	0.09	0.00	30.8	25.8	96.9

Table 3: SOLID vs. Dataset scales. ADR-Da. represents the ADR by DarkneTZ. Details are in Appendix C.6.

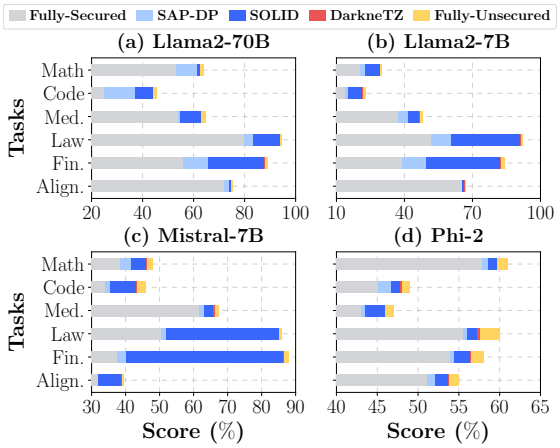

Figure 5: Customization performance comparison of secured models on six downstream tasks.

Obs5: The security of SOLID cannot be easily compromised by simply increasing the dataset scale. As shown in Table 3, the distillation ratios for SOLID increase marginally with larger datasets, showing only a 0.5% ADR rise when scaling from 51k to 500k samples. In contrast, DarkneTZ exhibits a significant increase in the ADR, from 86.5% to 96.9%, over the same dataset size range. This highlights the robustness of SOLID's security against increasing attack dataset sizes. Details of the attack datasets are provided in Appendix B.2.

Obs6: SOLID consistently outperforms baseline deployments in customization while achieving security levels comparable to fully-secured approaches. Its customization performance closely matches full parameter fine-tuning. As shown in Figure 5, SOLID improves scores in the Law domain by 10% over SAP-DP and fully-secured methods on Llama2-70B, and by 35% on 7B models. Similar trends are observed on Phi-2, though the gain in Law narrows to 1%. Additionally, the performance of SOLID consistently matches the performance of full parameter fine-

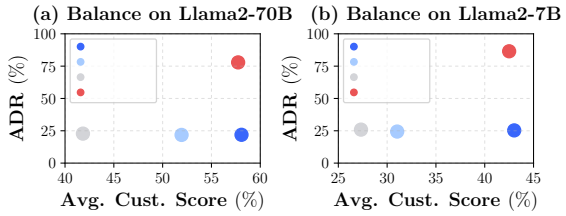

Figure 6: ADRs vs. average customization score. Points closer to the bottom-right indicate better balance.

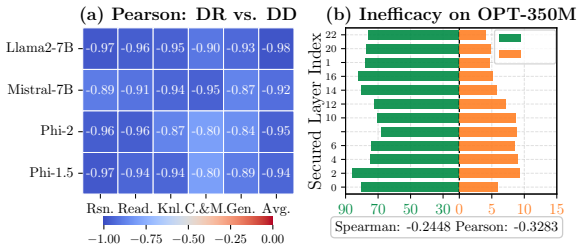

Figure 7: (a) presents the Pearson coefficient between distillation ratio (DR) and distillation difficulty (DD) across four models and six domains. (b) depicts the link between ADR and DD for Llama2-7B and OPT-350M.

tuning across four architectures, with differences within 4%. This indicates that securing a small subset of parameters preserves customization while ensuring strong protection against distillation attacks. Further results are in Appendix B.6 and C.3.

We summarize the security and customization performance of each deployment in Figure 6. SOLID achieves an optimal balance between distillation prevention and customization, outperforming other baselines. In the next subsection, we discuss how the distillation difficulty metric optimizes the security-customization trade-off.

4.5 Discussion on DD (RQ4)

We assess the efficacy of distillation difficulty (DD) in estimating distilled model performance by calculating the Pearson and Spearman correlation coefficients between DD and ADR across different domains. To address uncertainties regarding the effectiveness of DD in shallow transformers, we secure and attack 2-layer secured sets in OPT-350M (Zhang et al., 2022), which has 350M parameters. Based on the results shown in Figure 7, we have following observations.

Obs7: DD is effective in larger models, with a clear negative correlation between DD and average distillation ratios. As shown in Figure 7 (a), the Pearson coefficient for Llama2-7B consistently remains below -0.80, reaching as low as -0.98. We also observe similar phenomena in other models with varying architectures and sizes, confirming DD as a reliable predictor of distilles model performance and the effectiveness of SOLID. Results of Spearman coefficients are in Appendix B.9.

Obs8: DD is ineffective in smaller OPT model, with notable inconsistencies with ADRs. As shown in Figure 7 (b), DD exhibits weak negative correlation with ADR in OPT-350M (coefficients > -0.33), showing its unsuitability for predicting distillation performance. Additionally, optimal security is achieved by protecting the middle layers rather than the initial or output layers, making SOLID unable to identify the smallest secured set. Further details are provided in Appendix C.9.

5 Related Works

On-premises deployment. Using LLM services for customization poses significant privacy risks, as user data may be exposed during transmission, storage, and processing (Li et al., 2024c). To mitigate this, privacy-sensitive sectors require *on-premises deployment* of LLMs, which retains both data and models within their local infrastructure (Schillaci, 2024; Nevo et al., 2024). However, this shifts security risks to vendors, who lose control over model use and face increased threats of theft, especially from hardware- and communication-based attacks on GPUs (Nayan et al., 2024; Rakin et al., 2022). To secure models locally, hardware-based protections such as TrustZone have been proposed (Pinto and Santos, 2019; Zhang et al., 2024a; Li et al., 2024a), but they are resource-intensive with limited flexibility (Mo et al., 2020). A more adaptable approach is *layer-wise security*, which protects only selected layers (Lin et al., 2024; Chen et al., 2024; Zhang et al., 2024b). While prior work suggests securing shallow (Elgamal and Nahrstedt, 2020), intermediate (Shen et al., 2022), or output layers (Huang et al., 2024), most studies focus on smaller models. Our results show that securing a few, well-chosen bottom layers of LLMs can enhance security while preserving fine-tuning flexibility for on-premises deployment.

Model Distillation Attacks. Model distillation attacks allow adversaries to replicate model functionality using only black-box access, a process also known as functional extraction (Nevo et al., 2024; Xu et al., 2024a; Ezzeddine et al., 2024). While distillation attacks have been extensively studied in smaller models, such as CNNs (Orekondy et al., 2018), BERT (Sanh et al., 2020; Zanella-Beguelin et al., 2021), and ReLU-

based models (Canales-Martínez et al., 2024; Jagielski et al., 2020), their effectiveness against LLMs remains an open question. Our work extends these attacks to Llama2-70B and demonstrates that securing only the output layer remains insufficient to prevent near-complete functionality replication.

6 Conclusion

In this paper, we explore minimal secured sets to protect LLMs from query-based distillation attacks while preserving customization flexibility in on-premises deployments. We find that (1) distillation attacks targeting the secured top layer can successfully replicate the victim model, and (2) both the placement and number of secured layers introduce a security-customization trade-off. Based on these insights, we propose SOLID, a theoretically inspired deployment that optimizes this trade-off. Through extensive experiments, we show that SOLID balances security and customization effectively, outperforming baseline deployments, though it also has certain limitations.

Limitations

While our method effectively defends against distillation attacks and preserves model customization, it does not address other adversarial attacks in the black-box setting, such as membership inference attacks (MIA), as demonstrated in the Appendix B.10. To the best of our knowledge, this is the first work to explore a semi-open deployment framework for LLMs. However, the current algorithm still performs identification at the layer level and does not delve into the impact of different submodules within decoder layers on model security. Furthermore, our proposed metric exhibits reduced effectiveness when applied to smaller models, as discussed in Section 4.5. In future work, we aim to address these limitations by enhancing both the algorithm and the evaluation metric to improve the overall effectiveness of SOLID.

Acknowledgements

We are deeply grateful to the anonymous reviewers for their insightful comments and constructive suggestions, which significantly improved this work. We also acknowledge the support from the National Natural Science Foundation of China (No. 62306179, No.62472247 and No. 12326608); the National Key Research and Development Program of China(2024YFB3310000); Hetao Shenzhen-Hong Kong Science and Technology Innovation Cooperation Zone Project (No.HZQSWS-KCCYB-2024016); Guangdong Provincial Key Laboratory of Mathematical Foundations for Artificial Intelligence (2023B1212010001) and the Scientific Research Program of Shanghai Municipal Science and Technology Commission (24BC3200100).

References

Marah Abdin, Sam Ade Jacobs, Ammar Ahmad Awan, Jyoti Aneja, Ahmed Awadallah, Hany Awadalla, Nguyen Bach, Amit Bahree, Arash Bakhtiari, Harkirat Behl, and 1 others. 2024. Phi-3 technical report: A highly capable language model locally on your phone. *arXiv preprint arXiv:2404.14219*.

Martin Anthony, Peter L Bartlett, Peter L Bartlett, and 1 others. 1999. *Neural network learning: Theoretical foundations*, volume 9. cambridge university press Cambridge.

Jacob Austin, Augustus Odena, Maxwell Nye, Maarten Bosma, Henryk Michalewski, David Dohan, Ellen Jiang, Carrie Cai, Michael Terry, Quoc Le, and 1 others. 2021. Program synthesis with large language models. *arXiv preprint arXiv:2108.07732*.

Alexandre Bailly, Corentin Blanc, Élie Francis, Thierry Guillotin, Fadi Jamal, Béchara Wakim, and Pascal Roy. 2022. Effects of dataset size and interactions on the prediction performance of logistic regression and deep learning models. *Computer Methods and Programs in Biomedicine*, 213:106504.

Loubna Ben Allal, Niklas Muennighoff, Logesh Kumar Umapathi, Ben Lipkin, and Leandro von Werra. 2022. A framework for the evaluation of code generation models. https://github.com/bigcode-project/bigcode-evaluation-harness.

Yonatan Bisk, Rowan Zellers, Ronan Le Bras, Jianfeng Gao, and Yejin Choi. 2020. Piqa: Reasoning about physical commonsense in natural language. In *Thirty-Fourth AAAI Conference on Artificial Intelligence*.

Enric Boix-Adsera. 2024. Towards a theory of model distillation. *Preprint*, arXiv:2403.09053.

Isaac A Canales-Martínez, Jorge Chávez-Saab, Anna Hambitzer, Francisco Rodríguez-Henríquez, Nitin Satpute, and Adi Shamir. 2024. Polynomial time cryptanalytic extraction of neural network models. In *Annual International Conference on the Theory and Applications of Cryptographic Techniques*, pages 3–33. Springer.

Nicholas Carlini, Daniel Paleka, Krishnamurthy Dj Dvijotham, Thomas Steinke, Jonathan Hayase, A Feder Cooper, Katherine Lee, Matthew Jagielski, Milad Nasr, Arthur Conmy, and 1 others. 2024. Stealing

part of a production language model. *arXiv preprint arXiv:2403.06634*.

Sahil Chaudhary. 2023. Code alpaca: An instruction-following llama model for code generation. Accessed: 2024-09-23.

Mark Chen, Jerry Tworek, Heewoo Jun, Qiming Yuan, Henrique Ponde de Oliveira Pinto, Jared Kaplan, Harri Edwards, Yuri Burda, Nicholas Joseph, Greg Brockman, and 1 others. 2021. Evaluating large language models trained on code. *arXiv preprint arXiv:2107.03374*.

Yuxuan Chen, Rongpeng Li, Xiaoxue Yu, Zhifeng Zhao, and Honggang Zhang. 2024. Adaptive layer splitting for wireless llm inference in edge computing: A model-based reinforcement learning approach. *Preprint*, arXiv:2406.02616.

Zitao Chen and Karthik Pattabiraman. 2024. A method to facilitate membership inference attacks in deep learning models. *arXiv preprint arXiv:2407.01919*.

Hongjun Choi, Jayaraman J. Thiagarajan, Ruben Glatt, and Shusen Liu. 2024. Enhancing accuracy and parameter-efficiency of neural representations for network parameterization. *Preprint*, arXiv:2407.00356.

Christopher Clark, Kenton Lee, Ming-Wei Chang, Tom Kwiatkowski, Michael Collins, and Kristina Toutanova. 2019. Boolq: Exploring the surprising difficulty of natural yes/no questions. *arXiv preprint arXiv:1905.10044*.

Peter Clark, Isaac Cowhey, Oren Etzioni, Tushar Khot, Ashish Sabharwal, Carissa Schoenick, and Oyvind Tafjord. 2018. Think you have solved question answering? try arc, the ai2 reasoning challenge. *ArXiv*, abs/1803.05457.

Karl Cobbe, Vineet Kosaraju, Mohammad Bavarian, Jacob Hilton, Reiichiro Nakano, Christopher Hesse, and John Schulman. 2021. Training verifiers to solve math word problems. *Preprint*, arXiv:2110.14168.

Ganqu Cui, Lifan Yuan, Ning Ding, Guanming Yao, Bingxiang He, Wei Zhu, Yuan Ni, Guotong Xie, Ruobing Xie, Yankai Lin, Zhiyuan Liu, and Maosong Sun. 2024. Ultrafeedback: Boosting language models with scaled ai feedback. *Preprint*, arXiv:2310.01377.

Abhimanyu Dubey, Abhinav Jauhri, Abhinav Pandey, Abhishek Kadian, Ahmad Al-Dahle, Aiesha Letman, Akhil Mathur, Alan Schelten, Amy Yang, Angela Fan, and 1 others. 2024. The llama 3 herd of models. *arXiv preprint arXiv:2407.21783*.

Francisco Eiras, Aleksandar Petrov, Bertie Vidgen, Christian Schroeder, Fabio Pizzati, Katherine Elkins, Supratik Mukhopadhyay, Adel Bibi, Aaron Purewal, Csaba Botos, Fabro Steibel, Fazel Keshtkar, Fazl Barez, Genevieve Smith, Gianluca Guadagni, Jon Chun, Jordi Cabot, Joseph Imperial, Juan Arturo Nolazco, and 6 others. 2024. Risks and opportunities of open-source generative ai. *Preprint*, arXiv:2405.08597.

Tarek Elgamal and Klara Nahrstedt. 2020. Serdab: An iot framework for partitioning neural networks computation across multiple enclaves. In *2020 20th IEEE/ACM International Symposium on Cluster, Cloud and Internet Computing (CCGRID)*, pages 519–528. IEEE.

Fatima Ezzeddine, Omran Ayoub, and Silvia Giordano. 2024. Knowledge distillation-based model extraction attack using private counterfactual explanations. *arXiv preprint arXiv:2404.03348*.

Matthew Finlayson, Xiang Ren, and Swabha Swayamdipta. 2024. Logits of api-protected llms leak proprietary information. *arXiv preprint arXiv:2403.09539*.

Wenjie Fu, Huandong Wang, Chen Gao, Guanghua Liu, Yong Li, and Tao Jiang. 2023. Practical membership inference attacks against fine-tuned large language models via self-prompt calibration. *arXiv preprint arXiv:2311.06062*.

Leo Gao, Jonathan Tow, Baber Abbasi, Stella Biderman, Sid Black, Anthony DiPofi, Charles Foster, Laurence Golding, Jeffrey Hsu, Alain Le Noac'h, Haonan Li, Kyle McDonell, Niklas Muennighoff, Chris Ociepa, Jason Phang, Laria Reynolds, Hailey Schoelkopf, Aviya Skowron, Lintang Sutawika, and 5 others. 2023. A framework for few-shot language model evaluation.

Jianping Gou, Baosheng Yu, Stephen J Maybank, and Dacheng Tao. 2021. Knowledge distillation: A survey. *International Journal of Computer Vision*, 129(6):1789–1819.

Neel Guha, Julian Nyarko, Daniel Ho, Christopher Ré, Adam Chilton, Alex Chohlas-Wood, Austin Peters, Brandon Waldon, Daniel Rockmore, Diego Zambrano, and 1 others. 2024. Legalbench: A collaboratively built benchmark for measuring legal reasoning in large language models. *Advances in Neural Information Processing Systems*, 36.

Neel Guha, Julian Nyarko, Daniel E. Ho, Christopher Ré, Adam Chilton, Aditya Narayana, Alex Chohlas-Wood, Austin Peters, Brandon Waldon, Daniel N. Rockmore, Diego Zambrano, Dmitry Talisman, Enam Hoque, Faiz Surani, Frank Fagan, Galit Sarfaty, Gregory M. Dickinson, Haggai Porat, Jason Hegland, and 21 others. 2023. Legalbench: A collaboratively built benchmark for measuring legal reasoning in large language models. *Preprint*, arXiv:2308.11462.

Xuanli He, Lingjuan Lyu, Qiongkai Xu, and Lichao Sun. 2021. Model extraction and adversarial transferability, your bert is vulnerable! *arXiv preprint arXiv:2103.10013*.

Dan Hendrycks, Collin Burns, Steven Basart, Andy Zou, Mantas Mazeika, Dawn Song, and Jacob Steinhardt. 2021. Measuring massive multitask language understanding. *Proceedings of the International Conference on Learning Representations (ICLR)*.

Dan Hendrycks, Mantas Mazeika, and Thomas Woodside. 2023. An overview of catastrophic ai risks. *Preprint*, arXiv:2306.12001.

Edward J. Hu, Yelong Shen, Phillip Wallis, Zeyuan Allen-Zhu, Yuanzhi Li, Shean Wang, Lu Wang, and Weizhu Chen. 2021. Lora: Low-rank adaptation of large language models. *Preprint*, arXiv:2106.09685.

Xing Hu, Ling Liang, Shuangchen Li, Lei Deng, Pengfei Zuo, Yu Ji, Xinfeng Xie, Yufei Ding, Chang Liu, Timothy Sherwood, and 1 others. 2020. Deepsniffer: A dnn model extraction framework based on learning architectural hints. In *Proceedings of the Twenty-Fifth International Conference on Architectural Support for Programming Languages and Operating Systems*, pages 385–399.

Wei Huang, Yinggui Wang, Anda Cheng, Aihui Zhou, Chaofan Yu, and Lei Wang. 2024. A fast, performant, secure distributed training framework for llm. In *ICASSP 2024 - 2024 IEEE International Conference on Acoustics, Speech and Signal Processing (ICASSP)*, pages 4800–4804.

Arthur Jacot, Franck Gabriel, and Clément Hongler. 2018. Neural tangent kernel: Convergence and generalization in neural networks. *Advances in neural information processing systems*, 31.

Matthew Jagielski, Nicholas Carlini, David Berthelot, Alex Kurakin, and Nicolas Papernot. 2020. High accuracy and high fidelity extraction of neural networks. *Preprint*, arXiv:1909.01838.

Albert Q Jiang, Alexandre Sablayrolles, Arthur Mensch, Chris Bamford, Devendra Singh Chaplot, Diego de las Casas, Florian Bressand, Gianna Lengyel, Guillaume Lample, Lucile Saulnier, and 1 others. 2023. Mistral 7b. *arXiv preprint arXiv:2310.06825*.

Mandar Joshi, Eunsol Choi, Daniel S. Weld, and Luke Zettlemoyer. 2017. Triviaqa: A large scale distantly supervised challenge dataset for reading comprehension. In *Proceedings of the 55th Annual Meeting of the Association for Computational Linguistics*, Vancouver, Canada. Association for Computational Linguistics.

Tom Kwiatkowski, Jennimaria Palomaki, Olivia Redfield, Michael Collins, Ankur Parikh, Chris Alberti, Danielle Epstein, Illia Polosukhin, Jacob Devlin, Kenton Lee, and 1 others. 2019. Natural questions: a benchmark for question answering research. *Transactions of the Association for Computational Linguistics*, 7:453–466.

Taesung Lee, Benjamin Edwards, Ian Molloy, and Dong Su. 2018. Defending against machine learning model stealing attacks using deceptive perturbations. *arXiv preprint arXiv:1806.00054*.

Bas Lemmens and Roger Nussbaum. 2012. *Nonlinear Perron-Frobenius Theory*, volume 189. Cambridge University Press.

Ding Li, Ziqi Zhang, Mengyu Yao, Yifeng Cai, Yao Guo, and Xiangqun Chen. 2024a. Teeslice: Protecting sensitive neural network models in trusted execution environments when attackers have pre-trained models. *arXiv preprint arXiv:2411.09945*.

Qinbin Li, Junyuan Hong, Chulin Xie, Jeffrey Tan, Rachel Xin, Junyi Hou, Xavier Yin, Zhun Wang, Dan Hendrycks, Zhangyang Wang, Bo Li, Bingsheng He, and Dawn Song. 2024b. Llm-pbe: Assessing data privacy in large language models. *Preprint*, arXiv:2408.12787.

Qinbin Li, Junyuan Hong, Chulin Xie, Jeffrey Tan, Rachel Xin, Junyi Hou, Xavier Yin, Zhun Wang, Dan Hendrycks, Zhangyang Wang, and 1 others. 2024c. Llm-pbe: Assessing data privacy in large language models. *arXiv preprint arXiv:2408.12787*.

Yuanzhi Li, Sébastien Bubeck, Ronen Eldan, Allie Del Giorno, Suriya Gunasekar, and Yin Tat Lee. 2023. Textbooks are all you need ii: phi-1.5 technical report. *arXiv preprint arXiv:2309.05463*.

Zheng Lin, Guanqiao Qu, Xianhao Chen, and Kaibin Huang. 2024. Split learning in 6g edge networks. *Preprint*, arXiv:2306.12194.

Jinghua Liu, Yi Yang, Kai Chen, and Miaoqian Lin. 2024. Generating api parameter security rules with llm for api misuse detection. *arXiv preprint arXiv:2409.09288*.

Xiaogeng Liu, Nan Xu, Muhao Chen, and Chaowei Xiao. 2023. Autodan: Generating stealthy jailbreak prompts on aligned large language models. *arXiv preprint arXiv:2310.04451*.

Yu Meng, Mengzhou Xia, and Danqi Chen. 2024. Simpo: Simple preference optimization with a reference-free reward. *arXiv preprint arXiv:2405.14734*.

Todor Mihaylov, Peter Clark, Tushar Khot, and Ashish Sabharwal. 2018. Can a suit of armor conduct electricity? a new dataset for open book question answering. In *EMNLP*.

Shervin Minaee, Tomas Mikolov, Narjes Nikzad, Meysam Chenaghlu, Richard Socher, Xavier Amatriain, and Jianfeng Gao. 2024. Large language models: A survey. *Preprint*, arXiv:2402.06196.

Fan Mo, Ali Shahin Shamsabadi, Kleomenis Katevas, Soteris Demetriou, Ilias Leontiadis, Andrea Cavallaro, and Hamed Haddadi. 2020. Darknetz: towards model privacy at the edge using trusted execution environments. In *Proceedings of the 18th International Conference on Mobile Systems, Applications, and Services*, pages 161–174.

Subhabrata Mukherjee, Arindam Mitra, Ganesh Jawahar, Sahaj Agarwal, Hamid Palangi, and Ahmed Awadallah. 2023. Orca: Progressive learning from complex explanation traces of gpt-4. *arXiv preprint arXiv:2306.02707*.

Krishna Giri Narra, Zhifeng Lin, Yongqin Wang, Keshav Balasubramaniam, and Murali Annavaram. 2019. Privacy-preserving inference in machine learning services using trusted execution environments. *arXiv preprint arXiv:1912.03485*.

Tushar Nayan, Qiming Guo, Mohammed Al Duniawi, Marcus Botacin, Selcuk Uluagac, and Ruimin Sun. 2024. {SoK}: All you need to know about {On-Device}{ML} model extraction-the gap between research and practice. In *33rd USENIX Security Symposium (USENIX Security 24)*, pages 5233–5250.

Sella Nevo, Dan Lahav, Ajay Karpur, Yogev Bar-On, Henry-Alexander Bradley, and Jeff Alstott. 2024. *Securing AI model weights: Preventing theft and misuse of frontier models*. 1. Rand Corporation.

Tribhuvanesh Orekondy, Bernt Schiele, and Mario Fritz. 2018. Knockoff nets: Stealing functionality of black-box models. *Preprint*, arXiv:1812.02766.

Denis Paperno, Germán Kruszewski, Angeliki Lazaridou, Quan Ngoc Pham, Raffaella Bernardi, Sandro Pezzelle, Marco Baroni, Gemma Boleda, and Raquel Fernández. 2016. The lambada dataset.

Sandro Pinto and Nuno Santos. 2019. Demystifying arm trustzone: A comprehensive survey. *ACM computing surveys (CSUR)*, 51(6):1–36.

Pranav Rajpurkar, Robin Jia, and Percy Liang. 2018. Know what you don't know: Unanswerable questions for squad. *Preprint*, arXiv:1806.03822.

Adnan Siraj Rakin, Md Hafizul Islam Chowdhuryy, Fan Yao, and Deliang Fan. 2022. Deepsteal: Advanced model extractions leveraging efficient weight stealing in memories. In *2022 IEEE symposium on security and privacy (SP)*, pages 1157–1174. IEEE.

Keisuke Sakaguchi, Ronan Le Bras, Chandra Bhagavatula, and Yejin Choi. 2019. Winogrande: An adversarial winograd schema challenge at scale. *arXiv preprint arXiv:1907.10641*.

Victor Sanh, Lysandre Debut, Julien Chaumond, and Thomas Wolf. 2020. Distilbert, a distilled version of bert: smaller, faster, cheaper and lighter. *Preprint*, arXiv:1910.01108.

Zachary Schillaci. 2024. On-site deployment of llms. In *Large Language Models in Cybersecurity: Threats, Exposure and Mitigation*, pages 205–211. Springer Nature Switzerland Cham.

Tianxiang Shen, Ji Qi, Jianyu Jiang, Xian Wang, Siyuan Wen, Xusheng Chen, Shixiong Zhao, Sen Wang, Li Chen, Xiapu Luo, and 1 others. 2022. {SOTER}: Guarding black-box inference for general neural networks at the edge. In *2022 USENIX Annual Technical Conference (USENIX ATC 22)*, pages 723–738.

Xicong Shen, Yang Liu, Huiqi Liu, Jue Hong, Bing Duan, Zirui Huang, Yunlong Mao, Ye Wu, and Di Wu. 2023. A split-and-privatize framework for large language model fine-tuning. *Preprint*, arXiv:2312.15603.

Chawin Sitawarin, Norman Mu, David Wagner, and Alexandre Araujo. 2024. Pal: Proxy-guided black-box attack on large language models. *arXiv preprint arXiv:2402.09674*.

Robin Staab, Mark Vero, Mislav Balunović, and Martin Vechev. 2023. Beyond memorization: Violating privacy via inference with large language models. *arXiv preprint arXiv:2310.07298*.

Mirac Suzgun, Nathan Scales, Nathanael Schärli, Sebastian Gehrmann, Yi Tay, Hyung Won Chung, Aakanksha Chowdhery, Quoc V Le, Ed H Chi, Denny Zhou, , and Jason Wei. 2022. Challenging big-bench tasks and whether chain-of-thought can solve them. *arXiv preprint arXiv:2210.09261*.

Manveer Singh Tamber, Jasper Xian, and Jimmy Lin. 2024. Can't hide behind the api: Stealing black-box commercial embedding models. *arXiv preprint arXiv:2406.09355*.

Rohan Taori, Ishaan Gulrajani, Tianyi Zhang, Yann Dubois, Xuechen Li, Carlos Guestrin, Percy Liang, and Tatsunori B. Hashimoto. 2023. Stanford alpaca: An instruction-following llama model. `https://github.com/tatsu-lab/stanford_alpaca`.

Hugo Touvron, Louis Martin, Kevin Stone, Peter Albert, Amjad Almahairi, Yasmine Babaei, Nikolay Bashlykov, Soumya Batra, Prajjwal Bhargava, Shruti Bhosale, and 1 others. 2023. Llama 2: Open foundation and fine-tuned chat models. *arXiv preprint arXiv:2307.09288*.

Florian Tramèr, Fan Zhang, Ari Juels, Michael K Reiter, and Thomas Ristenpart. 2016. Stealing machine learning models via prediction {APIs}. In *25th USENIX security symposium (USENIX Security 16)*, pages 601–618.

Jean-Baptiste Truong, Pratyush Maini, Robert J Walls, and Nicolas Papernot. 2021. Data-free model extraction. In *Proceedings of the IEEE/CVF conference on computer vision and pattern recognition*, pages 4771–4780.

Neng Wang, Hongyang Yang, and Christina Dan Wang. 2023a. Fingpt: Instruction tuning benchmark for open-source large language models in financial datasets. *arXiv preprint arXiv:2310.04793*.

Neng Wang, Hongyang Yang, and Christina Dan Wang. 2023b. Fingpt: Instruction tuning benchmark for open-source large language models in financial datasets. *Preprint*, arXiv:2310.04793.

Yizhong Wang, Yeganeh Kordi, Swaroop Mishra, Alisa Liu, Noah A Smith, Daniel Khashabi, and Hannaneh Hajishirzi. 2022. Self-instruct: Aligning language models with self-generated instructions. *arXiv preprint arXiv:2212.10560*.

Colin Wei, Jason D Lee, Qiang Liu, and Tengyu Ma. 2019. Regularization matters: Generalization and optimization of neural nets vs their induced kernel. *Advances in Neural Information Processing Systems*, 32.

Robert Wolfe, Isaac Slaughter, Bin Han, Bingbing Wen, Yiwei Yang, Lucas Rosenblatt, Bernease Herman, Eva Brown, Zening Qu, Nic Weber, and 1 others. 2024. Laboratory-scale ai: Open-weight models are competitive with chatgpt even in low-resource settings. In *The 2024 ACM Conference on Fairness, Accountability, and Transparency*, pages 1199–1210.

Canwen Xu, Daya Guo, Nan Duan, and Julian McAuley. 2023. Baize: An open-source chat model with parameter-efficient tuning on self-chat data. *arXiv preprint arXiv:2304.01196*.

Xiaohan Xu, Ming Li, Chongyang Tao, Tao Shen, Reynold Cheng, Jinyang Li, Can Xu, Dacheng Tao, and Tianyi Zhou. 2024a. A survey on knowledge distillation of large language models. *arXiv preprint arXiv:2402.13116*.

Zihao Xu, Yi Liu, Gelei Deng, Yuekang Li, and Stjepan Picek. 2024b. A comprehensive study of jailbreak attack versus defense for large language models. *Preprint*, arXiv:2402.13457.

Xiang Yue, Xingwei Qu, Ge Zhang, Yao Fu, Wenhao Huang, Huan Sun, Yu Su, and Wenhu Chen. 2023. Mammoth: Building math generalist models through hybrid instruction tuning. *arXiv preprint arXiv:2309.05653*.

Santiago Zanella-Beguelin, Shruti Tople, Andrew Paverd, and Boris Köpf. 2021. Grey-box extraction of natural language models. In *International Conference on Machine Learning*, pages 12278–12286. PMLR.

Rowan Zellers, Ari Holtzman, Yonatan Bisk, Ali Farhadi, and Yejin Choi. 2019. Hellaswag: Can a machine really finish your sentence? In *Proceedings of the 57th Annual Meeting of the Association for Computational Linguistics*.

Susan Zhang, Stephen Roller, Naman Goyal, Mikel Artetxe, Moya Chen, Shuohui Chen, Christopher Dewan, Mona Diab, Xian Li, Xi Victoria Lin, and 1 others. 2022. Opt: Open pre-trained transformer language models. *arXiv preprint arXiv:2205.01068*.

Xiang Zhang, Junbo Zhao, and Yann LeCun. 2016. Character-level convolutional networks for text classification. *Preprint*, arXiv:1509.01626.

Xinlu Zhang, Chenxin Tian, Xianjun Yang, Lichang Chen, Zekun Li, and Linda Ruth Petzold. 2023. Alpacare: Instruction-tuned large language models for medical application. *arXiv preprint arXiv:2310.14558*.

Zheng Zhang, Na Wang, Ziqi Zhang, Yao Zhang, Tianyi Zhang, Jianwei Liu, and Ye Wu. 2024a. Groupcover: A secure, efficient and scalable inference framework for on-device model protection based on tees. In *Proceedings of the 41st International Conference on Machine Learning*.

Ziqi Zhang, Chen Gong, Yifeng Cai, Yuanyuan Yuan, Bingyan Liu, Ding Li, Yao Guo, and Xiangqun Chen. 2024b. No privacy left outside: On the (in-) security of tee-shielded dnn partition for on-device ml. In *2024 IEEE Symposium on Security and Privacy (SP)*, pages 3327–3345. IEEE.

Wayne Xin Zhao, Kun Zhou, Junyi Li, Tianyi Tang, Xiaolei Wang, Yupeng Hou, Yingqian Min, Beichen Zhang, Junjie Zhang, Zican Dong, Yifan Du, Chen Yang, Yushuo Chen, Zhipeng Chen, Jinhao Jiang, Ruiyang Ren, Yifan Li, Xinyu Tang, Zikang Liu, and 3 others. 2023. A survey of large language models. *Preprint*, arXiv:2303.18223.

Wei Zhao, Zhe Li, Yige Li, Ye Zhang, and Jun Sun. 2024. Defending large language models against jailbreak attacks via layer-specific editing. *arXiv preprint arXiv:2405.18166*.

Lianmin Zheng, Wei-Lin Chiang, Ying Sheng, Siyuan Zhuang, Zhanghao Wu, Yonghao Zhuang, Zi Lin, Zhuohan Li, Dacheng Li, Eric P. Xing, Hao Zhang, Joseph E. Gonzalez, and Ion Stoica. 2023. Judging llm-as-a-judge with mt-bench and chatbot arena. *Preprint*, arXiv:2306.05685.

Tianyu Zheng, Ge Zhang, Tianhao Shen, Xueling Liu, Bill Yuchen Lin, Jie Fu, Wenhu Chen, and Xiang Yue. 2024a. Opencodeinterpreter: Integrating code generation with execution and refinement. *arXiv preprint arXiv:2402.14658*.

Tianyu Zheng, Ge Zhang, Tianhao Shen, Xueling Liu, Bill Yuchen Lin, Jie Fu, Wenhu Chen, and Xiang Yue. 2024b. Opencodeinterpreter: Integrating code generation with execution and refinement. *arXiv preprint arXiv:2402.14658*.

Difan Zou, Yuan Cao, Dongruo Zhou, and Quanquan Gu. 2020. Gradient descent optimizes over-parameterized deep relu networks. *Machine learning*, 109:467–492.

A Proof of Theorem 1

In this section, we prove Theorem 1. We first revisit the our model, present several important lemmas and finally present the proof. Additional explanatory remarks are included in Appendix A.5.

A.1 Model Overview

The distilled model $f(\mathbf{X};\boldsymbol{\theta})$ is structured as a sequence of L transformer layers,

$$f(\mathbf{X}) = \varphi_L \circ \varphi_{L-1} \circ \ldots \circ \varphi_{\alpha L+1} \circ \hat{\varphi}_{\alpha L} \circ_{\alpha L-1} \circ \ldots \circ \varphi_1(\mathbf{X}), \tag{2}$$

where $\mathbf{X} \in \mathbb{R}^{n\times d}$ represents the input, interpreted as an assembly of n tokens, each possessing d hidden dimensions. Each transformer layer, indexed by $1 \le i \le L$, is represented by φ_i, which maps $\mathbb{R}^{n\times d}$ to $\mathbb{R}^{n\times d}$ and can be defined as follows,

$$\varphi_i\left(\mathbf{X}; K_i, Q_i\right) = \left[\mathbf{I}_n + \operatorname{softmax}\left(\frac{\mathbf{X}Q_i(\mathbf{X}K_i)^\top}{\sqrt{d_Q}\|\mathbf{X}\|^2}\right)\right]\mathbf{X}, \tag{3}$$

where $Q_i \in \mathbb{R}^{d\times d_Q}$, $K_i \in \mathbb{R}^{d\times d_Q}$ represent projection parameter matrices. Here, the αL-th layer is the distilled layer and the others are the public layers. For simplicity, we use the function $\hat{\varphi}_{\alpha L}$ to denote mapping of the distilled layer, i.e., $\hat{\varphi}_{\alpha L}(\mathbf{X}) = \varphi_{\alpha L}(\mathbf{X}; \hat{K}_{\alpha L}, \hat{Q}_{\alpha L})$.

A.2 Bounds on Different Orthogonal Components

Lemma 1. *For any $1 \le l \le L$, $1 \le p \le d$, any $\mathbf{X} \in \mathbb{R}^{n\times d}$, we have*

$$\begin{aligned}&\max_{\boldsymbol{v}:\|\boldsymbol{v}\|_2=1, \boldsymbol{v}\perp\mathbb{I}_n} \left|\boldsymbol{v}^\top \varphi_l\left(\mathbf{X}; K_l, Q_l\right)[p]\right| \\ &\qquad \le (1+\beta_D) \max_{\boldsymbol{v}:\|\boldsymbol{v}\|_2=1, \boldsymbol{v}\perp\mathbb{I}_n} \left|\boldsymbol{v}^\top \mathbf{X}[p]\right|\end{aligned} \tag{4}$$

where $\mathbb{I}_n$ is a column vector with dimensions $n\times 1$ and each element is 1, $\mathbf{X}[p]$ is the p-th column of the input $\mathbf{X}$, $\varphi_l\left(\mathbf{X}; K_l, Q_l\right)[p]$ is the p-th column of the l-th self-attention output, the coefficient β_D satisfies $0 < \beta_D < 1$ and it is related to the upper bound of the L2-norm of matrices K_l, Q_l.

Proof. Let $\boldsymbol{u} = \left\{\boldsymbol{u}_{l,1} = \frac{\mathbb{I}_n}{\sqrt{n}}, \boldsymbol{u}_{l,2}, \ldots, \boldsymbol{u}_{l,n}\right\}$ denote the eigenvectors of $\operatorname{softmax}\left(\frac{\mathbf{X}Q_l(\mathbf{X}K_l)^\top}{\sqrt{d_Q}\|\mathbf{X}\|^2}\right)$. Assume $\sigma_{l,1}, \sigma_{l,2}, \ldots, \sigma_{l,n}$ denote the eigenvalues of $\operatorname{softmax}\left(\frac{\mathbf{X}Q_i(\mathbf{X}K_i)^\top}{\sqrt{d_Q}\|\mathbf{X}\|^2}\right)$ and $-1 < \sigma_{l,n} < \beta_D$ for any l, n. Thus we have

$$\begin{aligned}
&\boldsymbol{v}^\top \varphi_l\left(\mathbf{X}; K_l, Q_l\right)[p] && (5a)\\
&= \boldsymbol{v}^\top \left[\mathbf{I}_n + \operatorname{softmax}\left(\frac{\mathbf{X}Q_l(\mathbf{X}K_l)^\top}{\sqrt{d_Q}\|\mathbf{X}\|^2}\right)\right]\mathbf{X}[p] && (5b)\\
&= \boldsymbol{v}^\top \left[\mathbf{I}_n + \operatorname{softmax}\left(\frac{\mathbf{X}Q_l(\mathbf{X}K_l)^\top}{\sqrt{d_Q}\|\mathbf{X}\|^2}\right)\right]\sum_{k=1}^{n}\alpha_{pk}\boldsymbol{u}_{l,k} && (5c)\\
&= \boldsymbol{v}^\top \sum_{k=1}^{n}\alpha_{pk}(1+\sigma_{l,k})\boldsymbol{u}_{l,k} && (5d)\\
&\le \max_{\boldsymbol{v}:\|\boldsymbol{v}\|_2=1, \boldsymbol{v}\perp\mathbb{I}_n} \left|\sum_{k=2}^{n}\alpha_{pk}(1+\sigma_{l,k})\boldsymbol{v}^\top u_{l,k}\right| && (5e)\\
&= \left\|\sum_{k=2}^{n}\alpha_{pk}(1+\sigma_{l,k})\boldsymbol{u}_{l,k}\right\|_2 && (5f)\\
&= \left[\sum_{k=2}^{n}\alpha_{pk}^2(1+\sigma_{l,k})^2\right]^{1/2} && (5g)\\
&\le (1+\beta_D) \max_{\boldsymbol{v}:\|\boldsymbol{v}\|_2=1, \boldsymbol{v}\perp\mathbb{I}_n} \left|\boldsymbol{v}^\top \mathbf{X}[p]\right|, && (5h)
\end{aligned}$$

where

$$\begin{aligned}\beta_D &= \max_{\substack{\|K_l\|_2\le D,\\ \|Q_l\|_2\le D}} \max_{\substack{\boldsymbol{v}:\|\boldsymbol{v}\|_2=1,\\ \boldsymbol{v}\perp\mathbb{I}_n}} \left\|\operatorname{softmax}\left(\frac{\mathbf{X}Q_l(\mathbf{X}K_l)^\top}{\sqrt{d_Q}\|\mathbf{X}\|^2}\right)\boldsymbol{v}\right\|_2 \\ &< 1\end{aligned}$$

The equation (5d) is due to $\boldsymbol{u}_{l,k}$ are the eigenvectors of $\operatorname{softmax}\left(\frac{\mathbf{X}Q_l(\mathbf{X}K_l)^\top}{\sqrt{d_Q}\|\mathbf{X}\|^2}\right)$. The inequality (5f) is because when $\boldsymbol{v} = \frac{\sum_{k=2}^{n}\alpha_{pk}(1+\sigma_{l,k})\boldsymbol{u}_{l,k}}{\left\|\sum_{k=2}^{n}\alpha_{pk}(1+\sigma_{l,k})u_{l,k}\right\|_2}$, we have the maximum value. □

Lemma 2. *For any $K_l, Q_l \in \mathbb{R}^{d\times s}$ and any $\mathbf{X} \in \mathbb{R}^{n\times d}$, the following equation always holds:*

$$\left|\mathbb{I}_n^\top \varphi_i\left(\mathbf{X}; K_i, Q_i\right)[p]\right| = 2\left|\mathbb{I}_n^\top \mathbf{X}[p]\right|, \tag{6}$$

where $\mathbf{X}[p]$ is the p-th column of the input $\mathbf{X}$, $\varphi_i\left(\mathbf{X}; K_i, Q_i\right)[p]$ is the p-th column of the l-th self-attention output.

Proof. Assume that a set of orthogonal basis for $\mathbb{R}^n$ is $\{\boldsymbol{u_1}, \boldsymbol{u_2}, \ldots, \boldsymbol{u_n}\}$, where $\boldsymbol{u_1} = \frac{\mathbb{I}_n}{\sqrt{n}}$. Then we can rewrite $\mathbf{X}[p]$ as $\mathbf{X}[p] = \sum_{j=1}^{n}\alpha_{pj}\boldsymbol{u_j}$, where $\alpha_{pj}(1 \le p \le d)$ are the corresponding coefficients for the p-th column of $\mathbf{X}$ under the orthogonal basis. Next, we calculate $\left|\mathbb{I}_n^\top f(\mathbf{X})[p]\right|$ and $\left|\mathbb{I}_n^\top \mathbf{X}[p]\right|$, respectively. Note that $\mathbb{I}_n^\top \boldsymbol{u_j} = 0$ for all $j \ne 1$. Therefore, we can obtain that,

$$\mathbb{I}_n^\top \mathbf{X}[p] = \sqrt{n}\alpha_{p1}. \tag{7}$$

Then we can get

$$\left|\mathbb{I}_n^\top \mathbf{X}[p]\right| = |\sqrt{n}\alpha_{p1}|. \tag{8}$$

Let $\sigma_{i1}, \sigma_{i2}, \ldots, \sigma_{in}$ denote the eigenvalues of $\operatorname{softmax}\left(\frac{\mathbf{X}Q_i(\mathbf{X}K_i)^\top}{\sqrt{d_Q}\|\mathbf{X}\|^2}\right)$. Applying the Perron–Frobenius theorem for Markov matrices (Lemmens and Nussbaum, 2012), we deduce that for the matrix $\operatorname{softmax}\left(\frac{\mathbf{X}Q_l(\mathbf{X}K_i)^\top}{\sqrt{d_Q}\|\mathbf{X}\|^2}\right)$, there exists only one eigenvalue equal to 1, while all other eigenvalues in absolute value are strictly less than 1. Without loss of generality, we assume $\sigma_{i1} = 1$, implying $|\sigma_{ij}| < 1$ for $j \neq 1$. Recalling the definition of $\varphi_i(\mathbf{X}; K_i, Q_i)$ and considering the linear operation, we can rewrite it as follows:

$$\varphi_i(\mathbf{X}; K_i, Q_i)[p] = \sum_{j=1}^{n} \alpha_{pj}(1+\sigma_{ij})\boldsymbol{u_j}. \tag{9}$$

Then we calculate the term $|\mathbb{I}_n^\top \varphi_i(\mathbf{X}; K_i, Q_i)[p]|$ as follows,

$$\begin{aligned}
\left|\mathbb{I}_n^\top \varphi_i(\mathbf{X}; K_i, Q_i)[p]\right| &= \left|\mathbb{I}_n^\top \Big(\sum_{j=1}^{n} \alpha_{pj}(1+\sigma_{ij})\boldsymbol{u_j}\right| && \text{(10a)}\\
&= \left|\sqrt{n}\left(\alpha_{p1}(1+\sigma_{i1})\right)\right| && \text{(10b)}\\
&= 2|\sqrt{n}\alpha_{p1}|, && \text{(10c)}
\end{aligned}$$

where (10a) is induced by substituting the equation (9) into $\left|\mathbb{I}_n^\top \varphi_i(\mathbf{X}; K_i, Q_i)[p]\right|$, (10b) is due to $\mathbb{I}_n^\top \boldsymbol{u_j} = 0$ for all $j \neq 1$, (10c) follows the fact that $\sigma_{i1} = 1$.

□

A.3 Proof of Theorem 1

We first prove the following result. For simplicity of notations, we use $f(\mathbf{X})[p]$ to denote the p-th ($1 \leq p \leq d$) column of the the distilled model $f(\mathbf{X})$, where the parameters in the αL-th layer is replaced with the matrices $\hat{K}_{\alpha L}$ and $\hat{Q}_{\alpha L}$. We use the function $\hat{\varphi}_{\alpha L}(\mathbf{X}) = \varphi_{\alpha L}(\mathbf{X}; \hat{K}_{\alpha L}, \hat{Q}_{\alpha L})$ to denote the mapping of the (αL)-th layer. Then we are going to show that there exists $\alpha^\star = \log_2 \frac{2}{1+\beta_D}$ and $0 < \beta_D < 1$ makes the following equations hold.

(1) Assume $\alpha < \alpha^\star$. For any $\mathbf{X}$, $\|K_i\|_2 \leq D, \|Q_i\|_2 \leq D$, there exists a zero measure set $\mathcal{K}(\mathbf{X})$ and $\mathcal{Q}(\mathbf{X})$ such that

$$\lim_{L\to\infty} \left\| \frac{f(\mathbf{X})[p]}{\|f(\mathbf{X})[p]\|_2} - \frac{\mathbb{I}_n}{\sqrt{n}} \right\|_2 = 0. \tag{11}$$

(2) For any $\alpha > \alpha^\star$, there exists a sequence of matrix $\{K_i, Q_i\}_{i\geq 1}$ such that for any distilled matrix $K_{\alpha L}$ and $Q_{\alpha L}$, we have $\|K_i\|_2 \leq D, \|Q_i\|_2 \leq D$, we have,

$$\lim_{L\to\infty} \left\| \frac{f(\mathbf{X})[p]}{\|f(\mathbf{X})[p]\|_2} - \frac{\mathbb{I}_n}{\sqrt{n}} \right\|_2 = \sqrt{2}. \tag{12}$$

Proof. Based on Lemma (1), we obtain that

$$\begin{aligned}
&\max_{\boldsymbol{v}:\|\boldsymbol{v}\|_2=1,\, \boldsymbol{v}\perp\mathbb{I}_n} \left|\boldsymbol{v}^\top f(\mathbf{X})[p]\right| \\
&\leq (1+\beta)^L \max_{\boldsymbol{v}:\|\boldsymbol{v}\|_2=1,\, \boldsymbol{v}\perp\mathbb{I}_n} \left|\boldsymbol{v}^\top \mathbf{X}[p]\right|.
\end{aligned} \tag{13}$$

Based on Lemma (2), we know that

$$\begin{aligned}
&\left|\mathbb{I}_n^\top f(\mathbf{X})[p]\right| \\
&= 2^{(1-\alpha)L-1} \left|\mathbb{I}_n^\top \hat{\varphi}_{\alpha L} \circ \varphi_{\alpha L-1} \circ \cdots \circ \varphi_1(\mathbf{X})[p]\right|.
\end{aligned} \tag{14}$$

We firstly prove the equation (11). When

$$\left|\mathbb{I}_n^\top f(\mathbf{X})[p]\right| \neq 0, \tag{15}$$

then we have

$$\begin{aligned}
&\left\| \frac{f(\mathbf{X})[p]}{\|f(\mathbf{X})[p]\|_2} - \frac{\mathbb{I}_n}{\sqrt{n}} \right\|_2 && \text{(16a)}\\
&= \left[2 - \frac{2\mathbb{I}_n^\top f(\mathbf{X})[p]}{\sqrt{n}\sqrt{\frac{(\mathbb{I}_n^\top f(\mathbf{X})[p])^2}{n} + (\boldsymbol{v}^\top f(\mathbf{X})[p])^2)}}\right]^{1/2} && \text{(16b)}\\
&= \sqrt{2}\left[1 - \frac{1}{\sqrt{1 + \frac{n(\boldsymbol{v}^\top f(\mathbf{X})[p])^2}{(\mathbb{I}_n^\top f(\mathbf{X})[p])^2}}}\right]^{1/2} && \text{(16c)}\\
&\leq \sqrt{2}\left[1 - \frac{1}{\sqrt{1 + \frac{n(1+\beta)^{2L}|\boldsymbol{v}^\top \mathbf{X}[p]|^2}{2^{2[(1-\alpha)L-1]}\left|\mathbb{I}_n^\top \hat{\varphi}_{\alpha L} \circ \cdots \circ \varphi_1(\mathbf{X})[p]\right|^2}}}\right]^{1/2} && \text{(16d)}\\
&\leq 2\sqrt{2n}\left(\frac{1+\beta}{2^{1-\alpha}}\right)^L \frac{\left|\boldsymbol{v}^\top \mathbf{X}[p]\right|}{\left|\mathbb{I}_n^\top \hat{\varphi}_{\alpha L} \circ \varphi_{\alpha L-1} \circ \cdots \circ \varphi_1(\mathbf{X})[p]\right|}, && \text{(16e)}
\end{aligned}$$

where the inequality (16d) is based on the inequality (13) and (14). The inequality (16e) is based on Lemma (3). Therefore, if $\alpha < \log_2 \frac{2}{1+\beta_D}$ and $\left|\mathbb{I}_n^\top f(\mathbf{X})[p]\right| \neq 0$, then we have $\lim_{L\to\infty}\left(\frac{1+\beta_D}{2^{1-\alpha}}\right)^L = 0$. Now we can consider when $\left|\mathbb{I}_n^\top f(\mathbf{X})[p]\right| = 0$. In fact, it is easy to show that this can only happens when $\hat{K}_{\alpha L}$ and $\hat{Q}_{\alpha L}$ belong to certain sets making $\left|\mathbb{I}_n^\top f(\mathbf{X})[p]\right| = 0$, which corresponds to zero measure set $\mathcal{K}(\mathbf{X})$ and $\mathcal{Q}(\mathbf{X})$ depending on the input $\mathbf{X}$. Since the input space is countable, therefore,

the union $\cup_{\mathbf{X}\in\mathcal{X}}\mathcal{K}(\mathbf{X})$ and $\cup_{\mathbf{X}\in\mathcal{X}}\mathcal{Q}(\mathbf{X})$ are also zero-measure sets.

To prove equation (12), let $K^\star$, $Q^\star$ with $\|K^\star\|_2 \le D, \|Q^\star\|_2 \le D$ satisfy the following condition,

$$\max_{\boldsymbol{v}:\|\boldsymbol{v}\|_2=1,\boldsymbol{v}\perp\mathbb{I}_n} \left\|\text{softmax}\left(\frac{\mathbf{X}Q_l(\mathbf{X}K_l)^\top}{\sqrt{d_Q}\|\mathbf{X}\|^2}\right)\boldsymbol{v}\right\|_2 = \beta_D. \tag{17}$$

Let $\boldsymbol{v}^\star$ be the solver of the above optimization problem (17) and consider the $K_l = K^\star$, $Q_l = Q^\star$ and $\mathbf{X}^\star = [\boldsymbol{v}^\star, \boldsymbol{v}^\star, \cdots, \boldsymbol{v}^\star]$. Clearly, $\boldsymbol{v}^\star \perp \mathbb{I}_n$. Assume there exists $\boldsymbol{u} : \|\boldsymbol{u}^\star\|_2 = 1$ satisfying $\boldsymbol{u}^\star \perp \mathbb{I}_n$, $\boldsymbol{u}^\star \perp \boldsymbol{v}^\star$, therefore we can rewrite $f(\mathbf{X}^\star)[p]$ as follows,

$$\begin{aligned} f(\mathbf{X}^\star)[p] = &\frac{\mathbb{I}_n^\top}{\sqrt{n}} f(\mathbf{X}^\star)\frac{\mathbb{I}_n}{\sqrt{n}} \\ &+ \boldsymbol{v}^{\star\top} f(\mathbf{X}^\star)\boldsymbol{v}^\star + \boldsymbol{u}^{\star\top} f(\mathbf{X}^\star)\boldsymbol{u}^\star. \end{aligned} \tag{18}$$

For any $1 \le l \le L$, based on Lemma (1), we know that

$$\left|\boldsymbol{v}^{\star\top} f(\mathbf{X}^\star)[p]\right| = (1+\beta_D)^L \left|\boldsymbol{v}^{\star\top}\mathbf{X}^\star[p]\right|. \tag{19}$$

Since

$$\left|\mathbb{I}_n^\top f(\mathbf{X}^\star)[p]\right| = 2^L \left|\mathbb{I}_n^\top \mathbf{X}^\star[p]\right| = |\mathbb{I}_n^\top \boldsymbol{v}^\star| = 0 \tag{20}$$

and

$$\left|\boldsymbol{v}^{\star\top} f(\mathbf{X}^\star)[p]\right| = (1+\beta_D)^L \left|\boldsymbol{v}^{\star\top}\mathbf{X}^\star[p]\right| \neq 0. \tag{21}$$

Then we have

$$\left\|\frac{f(\mathbf{X}^\star)[p]}{\|f(\mathbf{X}^\star)[p]\|_2} - \frac{\mathbb{I}_n}{\sqrt{n}}\right\|_2 \tag{22a}$$

$$= \left[2 - \frac{2\mathbb{I}_n^\top f(\mathbf{X}^\star)[p]}{\sqrt{n}\,\|f(\mathbf{X}^\star)[p]\|_2}\right]^{1/2} \tag{22b}$$

$$= \left[2 - \frac{2\mathbb{I}_n^\top}{\sqrt{n}} \cdot \frac{f(\mathbf{X}^\star)[p]}{\sqrt{\begin{array}{l}\frac{1}{n}\left(\mathbb{I}_n^\top f(\mathbf{X}^\star)[p]\right)^2 + \left(\boldsymbol{v}^{\star\top} f(\mathbf{X}^\star)[p]\right)^2 \\ + \left(\boldsymbol{u}^{\star\top} f(\mathbf{X}^\star)[p]\right)^2\end{array}}}\right]^{1/2} \tag{22c}$$

$$\ge \left[2 - \frac{2\mathbb{I}_n^\top}{\sqrt{n}} \frac{f(\mathbf{X}^\star)[p]}{\sqrt{\frac{1}{n}(\mathbb{I}_n^\top f(\mathbf{X}^\star)[p])^2 + (\boldsymbol{v}^{\star\top} f(\mathbf{X}^\star)[p])^2}}\right]^{1/2} \tag{22d}$$

$$= \left[2 - 2\frac{\frac{\mathbb{I}_n^\top f(\mathbf{X}^\star)[p]}{\sqrt{n}\left|\boldsymbol{v}^{\star\top} f(\mathbf{X}^\star)[p]\right|}}{\sqrt{1 + \frac{\left|\mathbb{I}_n^\top f(\mathbf{X}^\star)[p]\right|^2}{n\left|\boldsymbol{v}^{\star\top} f(\mathbf{X}^\star)[p])\right|^2}}}\right]^{1/2} \tag{22e}$$

$$= \left[2 - 2\frac{\frac{2^{(1-\alpha)L-1}\left|\mathbb{I}_n^\top \hat{\varphi}_{\alpha L}\circ\varphi_{\alpha L-1}\circ\cdots\circ\varphi_1(\mathbf{X}^\star)[p]\right|}{\sqrt{n}(1+\beta_D)^L\left|\boldsymbol{v}^{\star\top}\mathbf{X}^\star[p]\right|}}{\sqrt{1 + \frac{2^{2[(1-\alpha)L-1]}}{n(1+\beta_D)^{2L}}\frac{\left|\mathbb{I}_n^\top \hat{\varphi}_{\alpha L}\circ\varphi_{\alpha L-1}\circ\cdots\circ\varphi_1(\mathbf{X}^\star)[p]\right|^2}{\left|\boldsymbol{v}^{\star\top}\mathbf{X}^\star[p]\right|^2}}}\right]^{1/2} \tag{22f}$$

where equation (22c) is based on (18), equation (22f) is based on (21) and (14). When $\alpha > \log_2\frac{2}{1+\beta_D}$, we have $\lim_{L\to\infty}\left(\frac{2^{1-\alpha}}{1+\beta_D}\right)^L = 0$. Thus we have $\lim_{L\to\infty}\left\|\frac{f(\mathbf{X}^\star)[p]}{\|f(\mathbf{X}^\star[p]\|_2} - \frac{\mathbb{I}_n}{\sqrt{n}}\right\|_2 = \sqrt{2}$. This indicates that the p-th column of the output matrix $f(\mathbf{X}^\star)$ is not parallel to $\mathbf{I}_n$ for any p. This further indicates that the output matrix does not have the identical vector in each row. □

A.4 Technical Lemma

Lemma 3. *For any $x \in (0,1)$, it always holds* $\left[1 - \frac{1}{\sqrt{1+x^2}}\right]^{1/2} \le x$.

Proof. To establish the inequality $\left[1 - \frac{1}{\sqrt{1+x^2}}\right]^{1/2} \le x$, we begin by proving,

$$1 - \frac{1}{\sqrt{1+x^2}} \le x^2. \tag{23}$$

To demonstrate (23), we equivalently show

$$1 - x^2 \le \frac{1}{\sqrt{1+x^2}}. \tag{24}$$

Subsequently, it suffices to verify

$$(1-x^2)(\sqrt{1+x^2}) \le 1. \tag{25}$$

This is equivalent to proving

$$(1-x^2)^2(1+x^2) \le 1. \tag{26}$$

Thus, our focus shifts to demonstrating

$$(1-x^2)(1-x^4) \le 1. \tag{27}$$

Clearly, (27) holds true for any $x \in (0,1)$. □

A.5 Remarks

Remark 2: The existence of $\hat{f}_\infty(\mathbf{X})$ is a non-trivial result. While the mapping φ_i admits a fixed point at $\mathbf{X} = \mathbf{0}_{n\times d}$, the convergence of the iterative process governed by φ_i cannot be guaranteed using the contraction mapping theorem, as φ_i does not satisfy the contraction property for any pair (Q_i, K_i). This complexity becomes particularly evident in the special case where $n = 1$ and $\mathbf{X}$ is a column vector. Here, the output of φ_i satisfies the relation $\langle \mathbf{1}_d, \varphi_i(\mathbf{X}; K_i, Q_i)\rangle = 2\langle \mathbf{1}_d, \mathbf{X}\rangle$, implying that the iteration diverges unless $\mathbf{X}$ is orthogonal to $\mathbf{1}_d$. However, the divergence is not arbitrary; rather, the theorem reveals that it occurs

in a fixed, well-defined direction. This insight ensures the existence of a normalized output, which remains stable and meaningful despite the lack of strict convergence.

Remark 3: The existence of $\alpha^* \in (0, 1)$ is also a non-trivial statement, as α^* could potentially be zero, which would imply the absence of a critical layer such that securing layers prior to it guarantees the failure of the recovered model's functionality. The primary challenge lies in demonstrating that perturbations to the earlier layers result in rank-one outputs, a property that does not universally hold for arbitrary perturbations. To address this, we establish an alternative result: given an input matrix $\mathbf{X}$, rank-one outputs can be guaranteed if the perturbation matrices K_i and Q_i are chosen to avoid specific zero-measure sets, denoted as $\mathcal{K}(\mathbf{X})$ and $\mathcal{Q}(\mathbf{X})$, respectively. Assuming a countable domain $\mathcal{X} \times \mathcal{Y}$, which is typical for structured inputs such as sentences or images, it follows that the perturbation matrices to be avoided belong to the countable union of these sets, defined as $\mathcal{K} = \bigcup_{\mathbf{X} \in \mathcal{X}} \mathcal{K}(\mathbf{X})$ and $\mathcal{Q} = \bigcup_{\mathbf{X} \in \mathcal{X}} \mathcal{Q}(\mathbf{X})$. Since this union remains a zero-measure set, avoiding these specific sets ensures that the conditions of the theorem are satisfied for any input matrix $\mathbf{X}$.

B Experiment Details

To more intuitively compare the security differences between the SOLID method and a fully-secured approach, we define $\Delta\textbf{ADR}(I) = \text{ADR}(I) - \text{ADR}([L])$ to assess the resilience of the secured set I relative to the fully-secured approach. A smaller value of $\Delta\textbf{ADR}$ indicates resilience similar to that of the fully-secured model.

B.1 Model Details.

The foundation models we use in our experiments are selected from open-source repositories, and Table 4 shows the basic information of the models and their sources. Specifically, we employ Llama2-70B-chat[1] (Touvron et al., 2023), Llama2-7B-chat[2] (Touvron et al., 2023), and Mistral-7B-v0.1[3] (Jiang et al., 2023). For smaller models, we select Phi-2[4] (Abdin et al., 2024) and Phi-1.5[5] (Li et al., 2023). We also consider OPT model[6] (Zhang et al., 2022), which has only 350 million parameters and 24 decoder layers.

Model	Size	Decoder Layers
Llama2-70B-chat	70B	80
Llama2-7B-chat	7B	32
Mistral-7B-v0.1	7B	32
Phi-2	2.7B	32
Phi-1.5	1.3B	24
OPT	350M	24

Table 4: Model Info

B.2 Distillation Attacks.

Attack implementation details. In performing FT-all and FT-secure model distillation attacks, we adhere to the training hyper-parameters outlined in the Llama2 report (Touvron et al., 2023), employing the AdamW optimizer with a cosine learning rate scheduler. The initial learning rate is set to 2×10^{-5}, with a weight decay of 0.1, a batch size of 128, and bfloat16 precision for input sequences of 512 tokens. The LLaMA2-70B model is trained for 3 epochs with a random seed of 42, while other models are trained for 5 epochs across three seeds: 42, 1234, and 20. Despite limiting training to 3

[1]https://huggingface.co/meta-llama/Llama-2-70b-chat-hf
[2]https://huggingface.co/meta-llama/Llama-2-7b-chat-hf
[3]https://huggingface.co/mistralai/Mistral-7B-v0.1
[4]https://huggingface.co/microsoft/phi-2
[5]https://huggingface.co/microsoft/phi-1_5
[6]https://huggingface.co/facebook/opt-350m

epochs for the 70B model, the training loss stabilized effectively. Our implementation builds upon the llama-recipes repository provided by META.

For SEM attacks, distinct configurations were employed for SOLID and SAP-DP. In the case of SOLID, hidden representations from the secure-source components were collected and paired with the input data to train a substitute model. In contrast, for SAP-DP, representations from the sixth decoder layer and the model's final logits were utilized to construct the training dataset. In accordance with (Tamber et al., 2024), we applied a learning rate of 1.5e-4, a weight decay of 0.01, and a linear learning rate scheduler with 500 warmup steps. Both training and validation batch sizes were set to 32, with MSE as the loss function. SOLID was trained for 30 epochs due to its smaller model size, whereas SAP-DP was trained for 5 epochs.

All distillation experiments were conducted on Nvidia 4090 24G, 6000 Ada 48G, and A100 80G GPUs, utilizing PyTorch 2.2.0 and CUDA 11.8 on Ubuntu 20.04.6 LTS.

Base 51k Distillation Dataset. We ensure dataset coverage and reliability by using a 1:1 ratio of the MMLU [7] (Hendrycks et al., 2021) auxiliary training set and Alpaca dataset [8] (Taori et al., 2023), extracting 25.5k samples from each. From the MMLU auxiliary training data, we sample 50%, and from Alpaca, we use a step size of 2 to enhance diversity. The datasets are then formatted for model training, applying Alpaca and MMLU prompts from Table 5.

Extra Distillation Datasets. To enhance dataset diversity, the 100K, 200K, 300K, and 500K datasets integrate additional specialized sources. As detailed in Table 6, these sources include Baize (Xu et al., 2023) (158K English multi-turn conversations via ChatGPT's self-chat), MathInstruct (Yue et al., 2023) (260K curated math instruction instances focusing on hybrid reasoning), and OpenOrca (Mukherjee et al., 2023) (augmented FLAN collection with 1M GPT-4 completions and 3.2M GPT-3.5 completions). These enrichments are intended to support complex computational and theoretical tasks, offering broader topic coverage.

Validation Datasets. Table 7 outlines the composition of the validation datasets. For *Validation Dataset 1*, we extracted 50% from each of the 57 MMLU validation sub-datasets, totaling 1.5K instances, paired with Alpaca data selected using a step size of 751. This dataset is used with the 51K and 100K training sets. For larger training sets (200K, 300K, and 500K), *Validation Dataset 2* was created by adding 400 instances from three Baize subsets, expanding the validation set to 4.0K.

[7] https://github.com/hendrycks/test

[8] https://github.com/tatsu-lab/stanford_alpaca/blob/main/alpaca_data.json

B.3 Baselines.

In this section, we provide further details on the baselines used in our comparisons: SAP-DP and fully-secured. These schemes represent different strategies, each with distinct trade-offs in terms of customizability and security against model distillation attacks.

SAP. The Split-and-Privatize (SAP) framework (Shen et al., 2023) offers an approach to balance between protecting model privacy and data privacy while maintaining competitive performance. Specifically, the SAP framework keeps the bottom six encoder layers open, allowing user access and fine-tuning while securing the deeper layers on the vendor.

SAP-DP. To further strengthen protection while maintaining competitive performance, we extend SAP by incorporating differential privacy techniques by adding Laplace noise to perturb the logits during the fine-tuning process (Lee et al., 2018). The Laplace Distribution with mean μ and scale b is the distribution with probability density function:

$$\text{Laplace}(x|\mu, b) = \frac{1}{2b} \exp\left(-\frac{|x-\mu|}{b}\right)$$

Specifically, in SAP-DP, the noise n is sampled: $n \sim \text{Laplace}(0, 0.5)$ and added to the output logits of the model to balance privacy protection and model performance.

Fully-secured. Following (Eiras et al., 2024), we use the fully-secured approach as a baseline. This assumes the adversary has no access to internal model parameters, treating the model as a black-box, where only output data can be collected. We slightly broaden this setup by assuming the adversary knows the model's architecture but no other details. Thus, distilling the fully-secured model involves using the collected data to retrain a model with the same architecture to restore its general functionality.

DarkneTZ. Based on the work of (Mo et al., 2020), we use DarkneTZ as a baseline to test whether protecting only the output layers is sufficient to defend against distillation attacks. In this setup, we assume the adversary has no access to the

Dataset	Prompt Type	Description
Alpaca	with input	Below is an instruction that describes a task, paired with an input that provides further context. Write a response that appropriately completes the request.
	w/o input	Below is an instruction that describes a task. Write a response that appropriately completes the request.
MMLU	Question Answering	Below is a question with no choices. Write the correct answer that appropriately solves the question.
	Multiple Choice	The following is a multiple choice question, paired with choices. Answer the question in the format: "Choice:content".

Table 5: Prompts for Alpaca and MMLU auxiliary training data

Raw Data Set	51k	100k	200k	300k	500k
Alpaca	25.5	50	40	50	50
MMLU auxiliary training set	25.5	50	40	100	100
Baize-MedQuAD	0	0	40	50	50
Baize-Quora	0	0	40	50	50
Baize-Stackoverflow	0	0	40	50	50
MathInstruct	0	0	4	6	20
OpenOrca	0	0	0	0	180

Table 6: Composition of variously sized datasets

model parameters of the output layers, specifically the last decoder layer. Similar to the SAP framework, this approach allows the adversary to access and fine-tune all layers except the final decoder layer.

B.4 Implementation Details of SOLID.

Evaluation Datasets. We created a 1.5K Evaluation Set to assess model security under various secure-sourcing strategies. This set includes 50% of entries from each of the 57 MMLU validation sub-datasets (Hendrycks et al., 2021), distinct from Validation Set outlined in Table 7. Additionally, we selected an equal number of Alpaca dataset (Taori et al., 2023), using a step size of 751, ensuring no overlap with the Validation Set.

Hyper-parameter Sensitivity. As shown in Figure 8, we evaluate SOLID's sensitivity to tolerance magnitude ε, adjusting it from 0.05 to 1 in 0.05 increments while calculating the ΔADR for six distilled models. The results indicate that SOLID is minimally sensitive to changes in ε, with ΔADR values stabilizing as ε increases. This stability arises from the need for a smaller secured layer at higher ε, allowing the condition $R(I) \leq (1+\varepsilon)R([L])$ to be met with fewer layers. Additionally, the increase in ΔADR is smaller for larger models, suggesting that privatizing more parameters beyond a certain point offers diminishing returns in security.

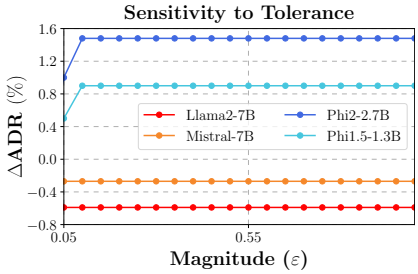

Figure 8: Sensitivity on ε.

B.5 Evaluation Benchmarks

Most of our evaluations are conducted using the lm-evaluation suite (Gao et al., 2023), the bigcode-evaluation-harness platform (Ben Allal et al., 2022), and MT-Bench (Zheng et al., 2023). For specific domains, such as finance and law, we utilize the official benchmark testing codes provided by their respective communities, as detailed below.

Evaluation on Customizabilities. We assess the customizability of models across six domains, as detailed in Table 8. Each domain includes specific benchmarks and metrics designed to evaluate different aspects of the model's performance in relation to customizability. In particular, for evaluating medical capabilities, we select two subcategories from the MMLU benchmark that are

Raw Data Set	Validation Set	Evaluation Set
Alpaca	765	765
MMLU auxiliary training set	751	751
Baize-MedQuAD	0	850
Baize-Quora	0	850
Baize-Stackoverflow	0	850
Total Length	1516	4066

Table 7: Composition of validation datasets of different sizes

related to the medical domain: *mmlu_anatomy* and *mmlu_professional_medicine*. For assessing legal reasoning, we select 10 multiple-choice and judgment-based subcategories from Legalbench. The performance of the model in these legal tasks is measured using perplexity, following the prompt structure provided by Legalbench. Specifically, the selected subcategories include:

- *cuad_audit_rights*
- *canada_tax_court_outcomes*
- *definition_classification*
- *cuad_affiliate_license-licensee*
- *learned_hands_business*
- *contract_nli_survival_of_obligations*
- *contract_nli_explicit_identification*
- *contract_nli_confidentiality_of_agreement*
- *hearsay*
- *contract_qa*

Evaluation on Security. We follow the Llama-2 report (Touvron et al., 2023) to evaluate the distilled model, including 16 benchmarks, which are categorized into 6 groups. Table 9 summarizes the functionality benchmarks used in our experiments, along with their test methods and performance metrics. Our model ranks choices in multiple-choice tasks and generates answers for open-ended generation tasks.

B.6 Model Customization

Datasets. To fine-tune the models for domain-specific tasks, we utilized several datasets tailored to different sectors, including Code (Zheng et al., 2024a), Math (Yue et al., 2023), Medical (Zhang et al., 2023), Finance (Wang et al., 2023a), Law (Guha et al., 2024), and Alignment (Meng et al., 2024). Table 10 lists the customization training datasets used in the experiments. For the code domain, we combine the datasets from CodeFeedback and CodeAlpaca. For law and finance, we merge all training datasets from Legalbench and FinGPT respectively. These datasets are then prepared for model training using the Alpaca prompts outlined in Table 5. Additionally, we randomly select 3,000 samples to serve as the validation dataset.

Customization Training Hyperparameters. In model customization, we use different hyperparameters depending on the model size. For LLaMA2-70B, we apply QLoRA with the settings outlined in Table 11, while for 7B models, we use LoRA. For smaller models like Phi2 and Phi-1.5, we fine-tune all model parameters. For LLaMA2-70B, we fine-tune it as a quantized 4-bit model over 1 epoch, starting with a learning rate of 1.5×10^{-6}. For the 7B models, we train for 3 epochs, with a seed value of 42. The training setup includes a weight decay of 0.1, a batch size of 128, a warmup ratio of 0.03, and input sequences of 512 tokens, following standard experimental practices (Hu et al., 2021). For Phi2 and Phi-1.5, we use the training hyperparameters from the LLaMA2 report. We employ the AdamW optimizer with a cosine learning rate scheduler, starting with a learning rate of 2×10^{-5}, a weight decay of 0.1, a batch size of 128, and use bfloat16 precision for 512-token input sequences. Specifically, for alignment, we follow SimPO (Meng et al., 2024) and set the preference parameters $\beta = 2$ and $\gamma = 1$. The learning rate is 1×10^{-6} for LLaMA2-70B and 5×10^{-7} for the 7B and smaller models. All experiments are conducted using the LLaMA-Factory on Nvidia 4090 24G, 6000 Ada 48G, and A100 80G GPUs, with PyTorch 2.2.0 and CUDA 11.8 on Ubuntu 20.04.6 LTS.

B.7 Security and Customization Transitions

For the LLaMA2-7B model, the smallest secure-source layer set identified by SOLID consists of a single decoder layer, whereas for Phi-2, it includes two decoder layers. Consequently, for LLaMA2-

Domain	Benchmark	Metric	n-shot	Reference
Code	HumanEval	Pass@1	0	(Chen et al., 2021)
	MBPP	Pass@1	1	(Austin et al., 2021)
Math	GSM8K	Exact Match	8	(Cobbe et al., 2021)
Medical	MMLU_Medical	Accuracy	5	(Hendrycks et al., 2021)
Finance	FPB	F1	0	(Wang et al., 2023b)
Law	LegalBench	Accuracy	0	(Guha et al., 2023)
Alignment	MT-Bench	Score	(GPT-4)	(Zheng et al., 2023)

Table 8: Details of the Six Customizability Benchmarks

Domain	Benchmark	Metric	n-shot	Reference
Commonsense Reasoning	PIQA	Accuracy	0	(Bisk et al., 2020)
	Hellaswag	Accuracy	0	(Zellers et al., 2019)
	Winogrande	Accuracy	0	(Sakaguchi et al., 2019)
	ARC_easy	Accuracy	0	(Clark et al., 2018)
	ARC_challenge	Accuracy	0	(Clark et al., 2018)
Reading Comprehension	OpenBookQ	Accuracy	0	(Mihaylov et al., 2018)
	LAMBADA	Accuracy	0	(Paperno et al., 2016)
	BoolQ	Accuracy	0	(Clark et al., 2019)
	SQuADv2	HasAns_EM	2	(Rajpurkar et al., 2018)
	SQuADv2	HasAns_F1	2	(Rajpurkar et al., 2018)
World Knowledge	NaturalQuestions	Exact Match	5	(Kwiatkowski et al., 2019)
	TriviaQA	Exact Match	5	(Joshi et al., 2017)
Code	HumanEval	Pass@1	0	(Chen et al., 2021)
	MBPP	Pass@1	1	(Austin et al., 2021)
Math	GSM8K	Exact Match	8	(Cobbe et al., 2021)
General Ability	MMLU	Accuracy	5	(Hendrycks et al., 2021)
	BBH	Accuracy	3	(Suzgun et al., 2022)

Table 9: Details of the Sixteen Functionality Benchmarks

7B, we opted to secure-source each even-indexed layer, while for Phi-2, we chose to secure-source non-overlapping pairs of layers (e.g., layers 0-1, 2-3). For each selected layer set, we first secure-source them, then subjected the semi-open model to FT-all attacks, and subsequently calculated the ΔADR of the layer set to assess its security.

When verifying the customization transition, due to computational constraints, we validated only every other layer set for both models (e.g., secure-source layers 0, 0-4, 0-8 ...). Specifically, we applied LoRA-based customization on LLaMA2-7B in the math domain, while for Phi-2, we utilized the full finetuning approach. The experimental hyperparameters remain consistent with those outlined in the Appendix B.6.

We further computed the ΔADR for each secure-source set within Mistral-7B-v0.1 and Phi-1.5. In these models, the smallest secure-source set identified by SOLID consists of one decoder layer and two decoder layers, respectively. Following the same experimental configuration as LLaMA2-7B and Phi-2, we secured each even-indexed layer for Mistral-7B, and non-overlapping pairs of layers for Phi-1.5. The complete results demonstrating the transition layers within the Mistral-7B and Phi-1.5 model that secure two non-overlapping consecutive layers are depicted in Figure 9. Once again, we observed a distinct presence of transition layers. Specifically, in Mistral-7B, the transition layer appears at the 24th layer, while in Phi-1.5, it is located within the first layer set. Further results for can be found in Appendix C.7.

B.8 Security Across Secure Sizes

To examine the influence of Secure layer size on model security, we conduct experiments on Secure-sourcing different amounts and proportions of pa-

Domain	Dataset Name	Size	Reference
Code	CodeFeedback	156k	(Zheng et al., 2024b)
	CodeAlpaca	20k	(Chaudhary, 2023)
Math	MathInstruction	262K	(Yue et al., 2023)
Medical	MedMCQA	183k	(Zhang et al., 2023)
Law	Legalbench	90k	(Guha et al., 2023)
Finance	FinGPT	204k	(Wang et al., 2023b)
Alignment	Ultrafeedback	62k	(Cui et al., 2024)

Table 10: Customization Training Datasets Composition

Model	Method	Rank r	Lora α	Dropout	Learning Rate	Epochs	Warmup R.
Llama2-70B	QLoRA	96	16	0.05	1.50E-04	1	0.03
Llama2-7B	LoRA	32	64	0.05	2.00E-05	3	0.03
Mistral-7B	LoRA	32	64	0.05	1.00E-06	3	0.03

Table 11: The Hyperparameters for Customization Training.

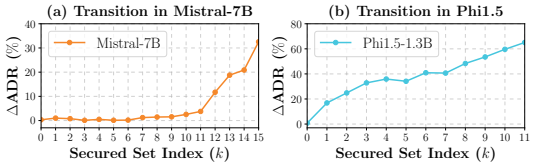

Figure 9: Security changes in Miatral-7B and Phi-1.5.

rameters in the model's decoder layer. We give instructions on the detailed setting of secured models in Table 12. The module names are all derived from the overall implementation functions of each model in the Transformers open-source repositories in Table 4. We utilize abbreviated module names to denote specific settings.

We further computed ΔADR by close-sourcing varying quantities and proportions of parameters under FT-all attacks on three additional models. As shown in Figure 10 and Figure 11(a), we observed the same pattern as with Llama2-7B, where security emerges once a sufficient number of parameters are secured. For example, on Mistral-7B, security occurs after secure-sourcing 100 million parameters, which is less than a single decoder layer. Secure-sourcing fewer parameters leads to a notable drop in security, with ΔADR rising to around 40%. Beyond this threshold, security stabilizes near 0% ΔADR. This pattern holds across all models, highlighting a critical threshold for effective secure-source. Furthermore, different architectures require varying secure-sourcing quantities to achieve security, even with similar model sizes. For instance, Mistral-7B reaches security by secure-sourcing 100 million parameters, Llama2-7B requires 200 million, and Phi-1.5 needs a higher rate of 7%, compared to 3% for Llama2-7B.

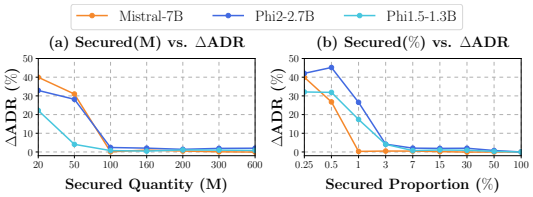

Figure 10: Δ ADR for different secure parameter quantities and proportions.

We explore how secured parameter ratio impacts the model security in Llama2-7B, as shown in Figure 11(b). For instance, technical skills such as Math show earlier transitions, with security emerging at 1% parameters secured, whereas domains such as Commonsense Reasoning require hiding 3%. In summary, secure-sourcing a small portion of parameters can provide sufficient security against model distillation, meanwhile, technical capabilities tend to be more challenging to distill than other domains.

B.9 Effectiveness of distillation difficulty

The complete Pearson and Spearman results are presented in Table 13, revealing a negative correlation between RS and the average distillation

		Llama-7B	Mistral-7B	Phi2-2.7B	Phi1.5-1.3B
Proportion	0.25%	W_k	W_q, W_k	W_k	W_k
	0.50%	W_q, W_k	W_o, MLP_{up}	W_q, W_k	W_q, W_k
	1%	W_q, W_k, W_v, W_o	W_q, W_k, W_v, W_o	W_q, W_k, W_v, W_d	$W_q, W_k, , W_v$
	3%	0	0	0	0
	7%	0-1	0-1	0-1	0-1
	15%	0-4	0-4	0-3	0-3
	30%	0-9	0-9	0-9	0-6
	50%	0-15	0-15	0-15,W_{em}	0-11,W_{em}
	100%	Fully-secured	Fully-secured	Fully-secured	Fully-secured
Quantity	20M	W_k	W_q, W_k	W_q, W_k, W_v	W_q, W_k, W_v, W_d
	50M	W_q, W_k, W_v	W_q, W_k, W_v, W_o	MLP	0
	100M	W_q, W_k, W_v, MLP	W_q, W_k, W_v, W_o, MLP	0, W_q, W_k, W_v	0-1
	160M	W_q, W_k, W_v, W_o, MLP	W_q, W_k, W_v, W_o, MLP	0-1	0-2
	200M	0	0	0-1, $W_q, W_k, W_v, W_d, MLP_{fl}$	0-3
	300M	0, W_q, W_v, W_o, MLP_{up}	0, W_q, W_v, W_o, MLP_{up}	0-3	0-5
	600M	0-2	0-2	0-7	0-11

Table 12: Secured Sizes Setting. "*" indicates an entire decoder layer.

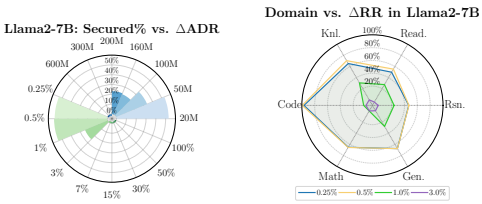

(a) Secured Ratio vs. ΔADR

(b) Secured Ratio vs. ΔDR

Figure 11: ΔADR and ΔDR changes in Llama2-7B with varying secured parameter ratios.

ratio. For example, in Llama2-7B, both Pearson and Spearman coefficients fall below -0.77. Similar trends are seen in models with varying architectures and sizes, confirming that RD is a reliable predictor of distilled model performance and demonstrating the effectiveness of SOLID. Additionally, Figure 12 shows scatter plots depicting the relationship between ΔADR and Distillation Difficulty(↑)s across four models, along with the corresponding Pearson and Spearman correlation coefficients. The Distillation Difficulty(↑)s were obtained from Section 4.3. As illustrated in Figure 12, we observe a clear trend: an increase in ΔADR corresponds to a decrease in model scores across all models analyzed. This inverse relationship is consistently supported by strong negative values for both Pearson and Spearman correlation coefficients, with the most significant negative correlation seen in Phi2-2.7B, indicating a substantial drop in model scores as ΔADR increases.

B.10 Adversarial Attack

In this section, we provide a detailed comparison of SOLID and SAP-DP in their effectiveness against three types of black-box adversarial attacks on the Llama2-7B model. The attacks considered include Membership Inference Attacks (MIA), Attribute Inference Attacks (AIA), and Prompt Injection Attacks (PIA).

Membership Inference Attack (MIA): This attack aims to determine whether a specific data point was included in the training dataset of the model. Attackers utilize model outputs to infer membership status, potentially exposing sensitive information about the training data (Fu et al., 2023; Chen and Pattabiraman, 2024). We conducted our experiment following SPV_MIA [9], which provides a robust framework for assessing model vulnerabilities. We focus on the AUC scores for SPV-MIA against semi-open models across Ag News datasets (Zhang et al., 2016).

Attribute Inference Attack (AIA): In this scenario, the adversary attempts to infer specific attributes of training data based on the model's outputs. This can lead to privacy breaches, particularly when sensitive attributes are involved (Staab et al., 2023; Li et al., 2024b). We conducted our experiments following the methodology outlined in (Staab et al., 2023) [10] and evaluated the top-3 accuracy on the PersonalReddit (PR) Dataset.

Prompt Injection Attack (PIA): This attack manipulates input prompts to coerce the model into producing desired outputs that may compromise the integrity or security of the system (Zhao et al., 2024; Xu et al., 2024b). In our experiment, we follow AutoDAN [11], which can automatically generate stealthy jailbreak prompts by the carefully designed hierarchical genetic algorithm.We evaluate the effectiveness of these prompts using the *keyword-based attack success rate* (ASR), which measures the presence of predefined keywords in responses generated LLMs. For gold stan-

[9] https://github.com/wjfu99/MIA-LLMs

[10] https://github.com/eth-sri/llmprivacy

[11] https://github.com/SheltonLiu-N/AutoDAN

Model	Rsn.	Read.	Knl.	Code & Math	Gen.	Avg.
Llama2-7B	-0.83 | -0.97	-0.77 | -0.96	-0.83 | -0.95	-0.85 | -0.90	-0.82 | -0.93	-0.80 | -0.98
Mistral-7B	-0.83 | -0.89	-0.82 | -0.91	-0.82 | -0.94	-0.78 | -0.95	-0.76 | -0.87	-0.87 | -0.92
Phi-2	-0.93 | -0.96	-0.84 | -0.96	-0.84 | -0.87	-0.84 | -0.80	-0.84 | -0.84	-0.87 | -0.95
Phi-1.5	-0.86 | -0.97	-0.78 | -0.94	-0.83 | -0.94	-0.90 | -0.80	-0.84 | -0.89	-0.80 | -0.94

Table 13: Correlation coefficients (Spearman | Pearson) between distillation ratio and distillation difficult.

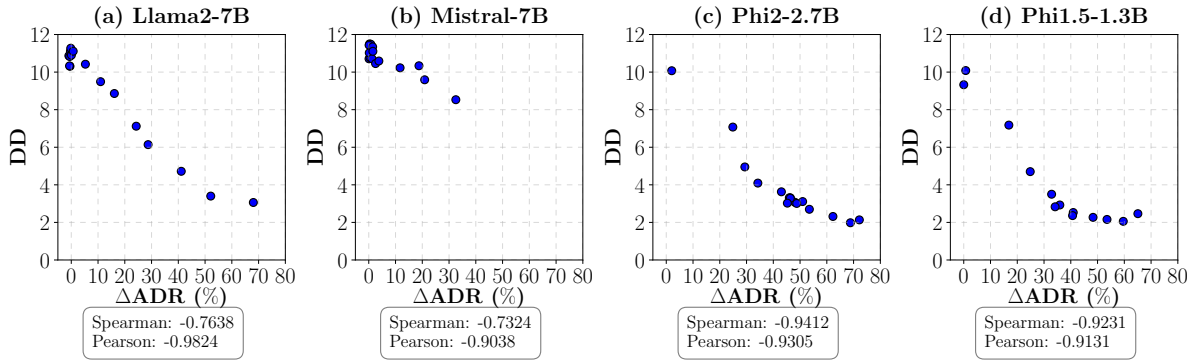

Figure 12: Correlation Analysis of ΔADR and Distillation Difficulty Across Different Models.

dard, LED [12], significantly enhances the security of LLMs against prompt injection attacks (PIA), reducing the ASR to 0.

Limited Defense against Adversarial Attack. We compare SOLID and SAP-DP in defending against three black-box adversarial attacks on Llama2-7B. Specifically, we apply the membership inference (Fu et al., 2023) (MIA), attribute inference (Staab et al., 2023) (AIA), and prompt injection (Liu et al., 2023) (PIA) attacks to the semi-open models produced by SAP-DP and SOLID. As shown in Table 14, we observe that SAP-DP outperforms SOLID across all three attacks, but still performs worse than the gold standard. This is because SOLID does not introduce additional output perturbation and thus provide limited defense against black-box adversarial attacks. Details can be found in Appendix B.10.

Approach	MIA↓	AIA↓	PIA↓
Gold Std.	58.0	43.9	0.00
SCARA	72.3	85.0	26.5
SAP-DP	72.2	83.9	24.9

Table 14: Performance of SCARA defending adversarial attacks. ↓ indicates the smaller the better.

[12]https://github.com/ledllm/ledllm

C Detailed Results

C.1 Comparison in two semi-open Llama2-70B

In this experiment, we examine two semi-open Llama2-70B models, where either the first two decoder layers are secure-source (referred to as Bottom2-Secured) or the last two decoder layers are secure-source (referred to as Top2-Secured). The objective is to compare their performance in terms of customization and their security under the distillation attack. The results are summarized in Table 15 and Table 16.

C.2 Evaluation Results under FT-all attack

In this section, we provide a comprehensive analysis of the evaluation results, comparing SOLID with two baseline methods: SAP-DP and a fully-secured approach. This comparison is conducted across 16 benchmarks under the FT-all attack scenario. The detailed results for Llama2-70B are presented in Table 17, while the results for Llama2-7B and Mistral-7B are shown in Table 18. Additionally, the outcomes for Phi-2 and Phi-1.5 are provided in Tables 19.

C.3 Customization Performance of Models

In this section, we present detailed evaluation results of the model customization performance across six downstream tasks used in our experi-

	Math	Code	Medical	Law	Finance	Alignment
Fully Secured	53.15	24.90	53.68	79.63	37.54	7.19
Bottom2-Secured	62.40	43.99	62.73	93.85	87.51	7.46
Top2-Secured	62.53	42.36	62.72	93.91	87.90	7.46

Table 15: Customization Performance of Llama2-70B under Different Secured Layers

	Benchmarks	Fully Secured	Semi-Open-1	Semi-Open-2
Rsn.	PIQA	50.82	50.49	79.05
	winogrande	51.07	51.22	72.93
	arc_easy	25.17	25.63	76.30
	arc_challenge	23.55	20.48	50.17
	Hellaswag	26.65	25.77	79.49
Read.	lambada	0.00	0.01	57.25
	BoolQ	43.30	37.92	84.95
	SQuADv2_EM	0.00	0.00	1.54
	SQuADv2_f1	0.23	1.01	35.59
	OBQA	25.60	24.40	44.00
Knl.	NQ	0.00	0.00	15.18
	TriviaQA	0.00	0.00	52.67
Code	mbpp	0.00	0.00	16.00
	HumanEval	0.00	0.00	13.41
Math	GSM8K	0.03	0.01	27.75
Gen.	MMLU	23.01	23.22	63.61
	BBH	0.00	0.00	49.45
Average Distillation Ratio(↓)		22.55	21.73	74.94

Table 16: Customization Performance of Llama2-70B under Different Secured Layers

ments. The detailed results for Llama2-70B are presented in Table 20, while the results for Llama2-7B and Mistral-7B are shown in Table 21 and Table 22. Additionally, the outcomes for Phi-2 and Phi-1.5 are provided in Tables 23 and Table 24.

C.4 Comparison in deployment baselines on llama2-70B

We compare the distillation security of SOLID with SAP-DP and Fully-secured as baselines under FT-secure and SEM attack strategies. The evaluation results on sixteen benchmarks are shown in Table 25.

C.5 Comparison in Distillation Attack Strategies

In this section, we present detailed evaluation results of the model distillation performance of SOLID under FT-secure and SEM attack strategies across six functionalities used in our experiments. The detailed results under the FT-secure distillation strategy are presented in Table 26. The results under SEM attack strategies are shown in Table 27.

C.6 Comparison in Distillation datasets scales

To investigate the impact of attack dataset scales on the efficiency of SOLID, we conduct model distillation attack on the Llama2-7B model using four different attack datasets of varying sizes: 100k, 200k, 300k, and 500k. The evaluation performance under different attack set scales are in Table 28

C.7 Transition Layer Results.

Security Performance. We close same-sized layer sets with different start points, and attack them using FT-all. Specifically, the sets consist of one layer for Llama2-7B (Table 29, Table 30), and two layers for Phi-2 (Table 33, Table 34). We further com-

		Pre-train	SOLID	SAP-DP	Fully-secured
Rsn.	PIQA	80.69	50.49	48.26	50.82
	Winogrande	74.74	51.22	50.59	51.07
	ARC-easy	80.35	25.63	26.35	25.17
	ARC-challenge	53.24	20.48	20.31	23.55
	Hellaswag	82.15	25.77	25.76	26.65
Read.	LAMBADA	75.07	0.01	0.00	0.00
	BoolQ	86.70	37.92	37.83	43.30
	SQuADv2_EM	51.23	0.00	0.00	0.00
	SQuADv2_f1	67.43	1.01	1.13	0.23
	OBQA	44.80	24.40	24.40	25.60
Knl.	NaturalQuestions	32.38	0.00	0.00	0.00
	TriviaQA	73.47	0.00	0.02	0.00
Code	MBPP	24.80	0.00	0.00	0.00
	HumanEval	25.00	0.00	0.00	0.00
Math	GSM8K	53.15	0.01	0.00	0.03
Gen.	MMLU	63.09	23.22	24.19	23.01
	BBH	61.40	0.00	0.00	0.00
Average Distillation Ratio(↓)		-	21.73	21.64	22.55

Table 17: Evaluation results of Llama2-70B under FT-all attack

puted the ΔADR for each secure-source set within Mistral-7B-v0.1 and Phi-1.5 in Appendix B.7. The results for the Mistral-7B-v0.1 model are presented in Table 31 and Table 32. Additionally, the performance outcomes for the Phi-1.5 model can be found in Table 35.

In all the above tables, "Pretrain" represents the model's original performance without any layers secured. These columns indicate the index of layers in the model that have been secured. "*" indicates fully-secured. All evaluation scores are averages from three different seed tests, corresponding to the values 20, 42, and 1234, following the details of the Sixteen Functionality Benchmarks in Appendix B.5.

Customizability Performance. We close varying numbers of layers from the start and fine-tune the open set, and then we observe the customizability transition in models. Table 36 shows the detailed evaluation results of Llama2-7B and Phi-2 on GSM8k benchmark.

C.8 Evaluation Results under Different Secure size

In this section, we present a comprehensive evaluation of the model's performance across sixteen benchmarks utilized in our experiments. The evaluation results for LLaMA2-7B, categorized by varying quantities and proportions of secure-source parameters, are displayed in Table 37 and Table 38, respectively. For the Mistral-7B model, the results are summarized in Table 39 and Table 40. Furthermore, the evaluation outcomes for the Phi-2 model can be found in Tables 41 and Table 42. The performance results for Phi-1.5 are also included in Tables 43 and Table 44 for comparison. For further details regarding the secure-source settings employed in our experiments, please refer to Appendix C.8.

C.9 Limitation on OPT-350M

To investigate the limitations of SOLID, we calculate the Distillation ratio of each secure-source set within the smaller model, OPT-350M (Zhang et al., 2022) with only 350M parameters. We set the secure-source set size to 2 and subsequently calculate ΔADRs for each secure-source set. The detailed results are shown in Figure 45.

		Llama2-7B			Mistral-7B		
		SOLID	**SAP-DP**	**Fully-secured**	**SOLID**	**SAP-DP**	**Fully-secured**
Rsn.	PIQA	49.56	49.56	49.47	51.63	50.22	49.35
	Winogrande	50.99	49.66	50.83	49.78	51.07	50.59
	ARC-easy	27.04	26.43	25.98	26.12	28.03	25.83
	ARC-challenge	21.07	20.56	22.47	19.94	21.42	22.35
	Hellaswag	25.56	25.69	26.39	26.10	25.97	25.39
Read.	LAMBADA	0.01	0.00	0.01	0.12	0.00	0.01
	BoolQ	44.30	41.70	48.34	39.05	37.83	45.80
	SQuADv2_EM	0.00	0.00	0.00	0.00	0.00	0.00
	SQuADv2_f1	0.49	0.63	0.59	1.21	0.26	0.66
	OBQA	25.13	23.00	25.93	25.60	25.20	25.00
Knl.	NaturalQuestions	0.01	0.01	0.04	0.00	0.00	0.02
	TriviaQA	0.00	0.00	0.02	0.00	0.00	0.01
Code	MBPP	0.00	0.00	0.00	0.00	0.00	0.00
	HumanEval	0.00	0.00	0.00	0.00	0.00	0.00
Math	GSM8K	0.00	0.00	0.00	0.00	0.00	0.00
Gen.	MMLU	24.26	22.92	24.45	25.24	23.05	23.26
	BBH	0.00	0.00	0.00	0.00	0.00	0.00
Average Distillation Ratio(↓)		25.03	24.16	25.62	22.41	22.28	22.68

Table 18: Evaluation results of 7B models under FT-all attack

		Phi-2			Phi-1.5		
		SOLID	**SAP-DP**	**Fully-secured**	**SOLID**	**SAP-DP**	**Fully-secured**
Rsn.	PIQA	54.17	52.01	52.07	53.43	52.61	50.44
	Winogrande	51.56	48.93	48.91	51.09	49.25	49.12
	ARC_easy	34.57	28.20	27.03	30.81	28.79	27.50
	ARC_challenge	19.45	19.37	18.66	20.56	19.80	21.22
	Hellaswag	27.61	25.32	25.26	26.27	25.66	25.05
	LAMBADA	0.75	0.02	0.00	0.59	0.00	0.00
Read.	BoolQ	45.29	40.21	44.60	46.98	41.80	46.28
	SQuADv2_EM	0.02	0.00	0.00	0.00	0.00	0.00
	SQuADv2_f1	2.61	0.28	0.64	0.78	0.65	1.60
	OBQA	24.80	26.60	25.80	26.60	28.60	26.87
Knl.	NaturalQuestions	0.00	0.00	0.02	0.04	0.00	0.00
	TriviaQA	0.01	0.00	0.01	0.01	0.00	0.00
Code	MBPP	0.00	0.00	0.00	0.00	0.00	0.00
	HumanEval	0.00	0.00	0.00	0.00	0.00	0.00
Math	GSM8K	0.00	0.00	0.00	0.00	0.00	0.00
Gen.	MMLU	24.16	22.87	22.95	24.07	22.95	22.95
	BBH	0.01	0.00	0.00	0.00	0.00	0.00

Table 19: Evaluation results of small models under FT-all attack

	Math	**Code**	**Medical**	**Law**	**Finance**	**Alignment**
Fully-Secure	53.15	24.90	53.68	79.63	55.63	7.19
SAP-DP	61.10	36.87	54.55	83.40	65.78	7.41
SOLID	62.40	43.99	62.73	93.85	87.51	7.46
Fully-Open	64.06	44.58	63.40	94.17	88.22	7.42

Table 20: Detailed results of Llama2-70B secure by SOLID on six downstream tasks.

	Math	Code	Medical	Law	Finance	Alignment
Fully-Secure	20.24	13.75	36.91	51.80	38.71	6.51
SAP-DP	20.24	13.75	36.91	51.80	38.71	6.52
SOLID	28.96	21.37	46.52	90.84	81.95	6.63
Fully-Open	29.34	21.265	47.60	90.49	84.09	6.63

Table 21: Detailed results of Llama2-7B secure by SOLID on six downstream tasks.

	Math	Code	Medical	Law	Finance	Alignment
Fully-Secure	38.21	33.83	61.50	50.47	37.39	3.20
SAP-DP	41.47	34.44	63.08	50.37	38.10	2.47
SOLID	46.10	43.16	66.78	84.94	86.19	3.87
Fully-Open	45.26	46.08	66.47	88.13	84.91	3.78

Table 22: Detailed results of Mistral-7B secure by SOLID on six downstream tasks.

	Math	Code	Medical	Law	Finance	Alignment
Fully-Secure	57.77	47.59	43.13	56.46	54.07	5.22
SAP-DP	58.52	46.65	43.40	56.81	54.37	5.11
SOLID	59.59	47.79	45.85	57.11	56.26	5.26
Fully-Open	59.60	48.40	45.93	57.19	56.68	5.27

Table 23: Detailed results of Phi-2 secure by SOLID on six downstream tasks.

	Math	Code	Medical	Law	Finance	Alignment
Fully-Secure	30.33	35.09	30.78	52.18	34.60	3.24
SAP-DP	30.25	35.45	32.66	51.99	34.27	3.68
SOLID	33.66	37.10	33.14	52.26	39.60	3.87
Fully-Open	34.49	37.45	33.23	52.34	39.90	3.68

Table 24: Detailed results of Phi-1.5 secure by SOLID on six downstream tasks.

		FT-secure		SEM	
		SOLID	SAP-DP	SOLID	SAP-DP
Rsn.	PIQA	49.78	49.40	48.62	49.00
	Winogrande	51.30	49.01	50.99	51.13
	ARC-easy	26.43	25.59	25.33	24.55
	ARC-challenge	21.41	21.42	22.01	20.93
	Hellaswag	26.07	26.10	25.90	25.22
Read.	LAMBADA	0.00	0.00	0.00	0.00
	BoolQ	45.09	37.83	44.95	39.80
	SQuADv2_EM	0.00	0.00	0.00	0.00
	SQuADv2_f1	0.98	1.01	0.59	1.00
	OBQA	24.40	23.80	25.03	22.96
Knl.	NaturalQuestions	0.00	0.00	0.00	0.00
	TriviaQA	0.00	0.00	0.00	0.00
Code	MBPP	0.00	0.00	0.00	0.00
	HumanEval	0.00	0.00	0.00	0.00
Math	GSM8K	0.00	0.00	0.00	0.00
Gen.	MMLU	23.18	23.66	22.98	22.83
	BBH	0.00	0.00	0.00	0.00
Average Distillation Ratio(↓)		22.60	21.80	22.40	22.30

Table 25: Evaluation results of Llama2-70B under FT-secure and SEM attack

		Llama2-7B	Mistral-7B	Phi-2	Phi-1.5
Rsn.	PIQA	49.95	49.55	54.57	52.45
	Winogrande	49.88	49.68	52.33	52.41
	ARC-easy	27.65	25.88	33.33	31.06
	ARC-challenge	20.81	22.69	19.03	18.77
	Hellaswag	26.04	25.01	27.62	26.88
Read.	LAMBADA	0.00	0.00	0.77	0.71
	BoolQ	38.13	46.01	44.34	57.49
	SQuADv2_EM	0.00	0.00	0.00	0.00
	SQuADv2_f1	0.22	0.36	3.07	2.27
	OBQA	25.70	25.12	24.40	25.20
Knl.	NaturalQuestions	0.00	0.00	0.00	0.00
	TriviaQA	0.00	0.00	0.01	0.00
Code	MBPP	0.00	0.00	0.00	0.00
	HumanEval	0.00	0.00	0.00	0.00
Math	GSM8K	0.00	0.00	0.00	0.00
Gen.	MMLU	24.23	23.56	23.03	24.10
	BBH	0.00	0.00	0.00	0.00
Average Distillation Ratio(↓)		24.80	22.50	23.56	26.97

Table 26: Distillation Performance of SOLID under FT-Secure attacks.

		Llama2-7B	Mistral-7B	Phi-2	Phi-1.5
Rsn.	PIQA	51.52	48.53	49.46	50.82
	Winogrande	50.28	51.02	48.70	50.59
	ARC-easy	24.83	25.83	25.93	24.62
	ARC-challenge	24.99	22.35	20.65	21.08
	Hellaswag	25.58	25.39	25.84	25.39
Read.	LAMBADA	0.00	0.01	0.00	0.01
	BoolQ	53.30	45.80	38.41	61.07
	SQuADv2_EM	0.00	0.00	0.00	0.00
	SQuADv2_f1	0.77	0.66	0.00	1.35
	OBQA	25.00	25.00	27.80	30.40
Knl.	NaturalQuestions	0.00	0.02	0.00	0.00
	TriviaQA	0.00	0.01	0.01	0.00
Code	MBPP	0.00	0.00	0.00	0.00
	HumanEval	0.00	0.00	0.00	0.00
Math	GSM8K	0.00	0.00	0.00	0.00
Gen.	MMLU	25.39	23.26	22.95	23.11
	BBH	0.00	0.00	0.00	0.00
Average Distillation Ratio(↓)		25.00	22.00	22.10	24.70

Table 27: Distillation Performance of SOLID under SEM attacks.

		51K	100K	200K	300K	500K
Rsn.	PIQA	49.56	49.89	49.18	49.18	49.59
	Winogrande	50.99	47.99	49.49	50.20	50.20
	ARC-easy	27.04	27.06	27.06	27.02	27.01
	ARC-challenge	21.07	21.33	20.90	21.16	21.48
	Hellaswag	25.56	26.49	26.46	26.50	26.19
Read.	LAMBADA	0.01	0.01	0.00	0.00	0.01
	BoolQ	44.30	44.41	44.10	44.07	44.96
	SQuADv2_EM	0.00	0.00	0.00	0.02	0.00
	SQuADv2_f1	1.05	0.32	0.51	0.52	0.71
	OBQA	25.13	25.00	23.80	25.20	25.60
Knl.	NaturalQuestions	0.01	0.08	0.08	0.06	0.06
	TriviaQA	0.00	0.02	0.01	0.03	0.01
Code	MBPP	0.00	0.00	0.00	0.00	0.00
	HumanEval	0.00	0.00	0.00	0.00	0.00
Math	GSM8K	0.00	0.00	0.00	0.00	0.00
Gen.	MMLU	24.26	25.34	25.43	26.14	26.41
	BBH	0.00	0.00	0.00	0.00	0.00
Average Distillation Ratio(↓)		25.07	25.03	24.89	25.26	25.48

Table 28: Evaluation Results of SOLID on Llama2-7B under Various Attack Set Scales.

		Pretrain	0	1	2	3	4	5	6	7
Rsn.	PIQA	76.66	49.56	51.43	49.53	50.45	49.84	50.27	50.96	51.09
	Hellaswag	75.45	25.56	25.75	25.88	26.16	25.91	27.20	29.39	28.89
	Winogrande	66.38	50.99	50.86	50.15	49.75	49.96	50.91	51.64	51.36
	ARC_easy	74.41	27.04	27.23	26.10	26.30	25.51	26.44	28.24	27.96
	ARC_challenge	44.11	21.07	20.31	20.19	21.30	22.04	21.56	20.62	22.92
Read.	OpenBookQA	68.49	0.01	0.11	0.02	0.02	0.01	0.00	0.05	0.04
	LAMBADA	80.67	44.30	41.22	38.36	41.43	38.08	38.14	38.40	41.55
	BoolQ	59.48	0.00	0.04	0.00	0.00	0.00	0.00	0.01	0.03
	SQuADv2_em	71.88	1.05	1.31	0.63	1.07	0.45	0.44	1.13	1.10
	SQuADv2_f1	43.80	25.13	24.60	23.60	24.93	25.67	24.47	25.07	26.00
Knl.	NaturalQuestions	22.47	0.01	0.00	0.01	0.03	0.02	0.01	0.13	0.08
	TriviaQA	57.23	0.00	0.01	0.00	0.02	0.01	0.01	0.07	0.10
Code	HumanEval	10.90	0.00	0.00	0.00	0.00	0.00	0.00	0.00	0.00
	MBPP	16.60	0.00	0.00	0.00	0.00	0.00	0.00	0.00	0.00
Math	GSM8K	20.24	0.00	0.00	0.00	0.00	0.00	0.00	0.00	0.00
Gen.	MMLU	45.83	24.26	25.37	23.98	24.26	24.75	24.01	25.23	27.45
	BBH	39.86	0.00	0.00	0.00	0.00	0.00	0.00	0.50	0.38
Avg. Performance Score(↓)		51.44	15.82	15.78	15.20	15.63	15.43	15.50	15.97	16.41
Average Distillation Ratio(↓)		-	30.76	30.67	29.55	30.39	29.99	30.13	31.04	31.90
Distillation Difficulty(↑)		-	11.11	11.27	10.87	10.31	10.83	10.33	10.90	11.11

Table 29: Evaluation Results of Llama2-7B under Different Secure Layers (Part1)

		16	18	20	22	24	26	28	30	*
Rsn.	PIQA	51.47	52.99	58.22	65.83	69.60	73.45	75.46	75.99	49.47
	Hellaswag	31.38	36.55	45.61	56.60	62.70	67.88	71.37	72.94	26.39
	Winogrande	53.09	55.98	58.96	64.12	64.80	65.25	65.46	66.53	50.83
	ARC_easy	30.58	35.35	43.85	55.92	62.56	68.36	70.85	72.60	25.98
	ARC_challenge	24.26	26.85	30.97	35.38	38.17	41.41	43.00	44.17	22.47
Read.	OpenBookQA	0.28	1.58	6.79	30.88	44.58	56.23	62.33	63.11	0.01
	LAMBADA	57.55	70.53	71.36	78.85	79.69	80.29	79.39	80.40	48.34
	BoolQ	0.08	0.90	2.34	7.07	6.04	6.87	3.54	9.46	0.00
	SQuADv2_em	2.21	13.48	21.47	35.72	36.96	39.32	37.08	42.08	0.59
	SQuADv2_f1	27.33	28.20	30.47	32.13	34.93	39.27	39.93	41.53	25.93
Knl.	NaturalQuestions	0.13	0.41	1.60	2.94	4.29	2.69	7.28	11.87	0.04
	TriviaQA	0.25	1.79	4.93	11.02	15.73	17.95	33.19	42.26	0.02
Code	HumanEval	0.00	0.00	0.00	0.00	0.00	3.25	8.34	10.98	0.00
	MBPP	0.00	0.00	0.00	0.07	0.47	2.27	8.80	13.27	0.00
Math	GSM8K	0.00	0.00	0.00	0.13	0.81	8.42	6.90	15.77	0.00
Gen.	MMLU	43.17	48.20	49.38	49.58	49.72	50.03	50.75	50.61	24.45
	BBH	0.76	11.44	19.79	28.87	31.16	35.98	38.24	40.54	0.00
Avg. Performance Score(↓)		18.97	22.60	26.22	32.65	35.42	38.76	41.29	44.36	16.15
Average Distillation Ratio(↓)		36.89	43.94	50.98	63.48	68.87	75.35	80.27	86.24	31.39
Distillation Difficulty(↑)		10.42	9.49	8.86	7.12	6.14	4.72	3.40	3.06	11.19

Table 30: Evaluation Results of Llama2-7B under Different Secured Layers (Part2). "*" indicates the fully secured model.

		Pretrain	0	1	2	3	4	5	6	7
Rsn.	PIQA	81.99	51.63	53.20	53.63	53.47	51.56	52.61	50.71	55.15
	Hellaswag	81.04	26.10	26.36	26.36	26.66	27.10	25.51	26.18	28.16
	Winogrande	74.03	49.78	49.78	51.01	50.38	49.91	50.14	49.70	51.17
	ARC_easy	80.77	33.03	31.96	30.71	29.66	30.25	30.35	26.44	32.38
	ARC_challenge	50.26	19.94	21.27	20.45	19.60	20.05	21.36	21.25	20.73
Read.	OpenBookQA	44.40	25.60	25.20	25.20	25.47	25.87	26.33	25.07	27.20
	LAMBADA	73.29	0.12	0.44	1.91	2.08	0.80	0.30	0.17	1.95
	BoolQ	83.67	39.05	53.12	45.95	38.61	47.35	38.06	46.44	47.66
	SQuADv2_em	64.04	0.00	0.00	0.01	0.01	0.01	0.00	0.00	0.01
	SQuADv2_f1	71.37	1.21	0.84	1.05	1.03	1.27	0.43	0.07	0.86
Knl.	NaturalQuestions	28.98	0.00	0.01	0.00	0.04	0.01	0.00	0.02	0.07
	TriviaQA	70.79	0.00	0.00	0.02	0.01	0.01	0.01	0.00	0.16
Code	HumanEval	29.88	0.00	0.00	0.00	0.00	0.00	0.00	0.00	0.00
	MBPP	38.40	0.00	0.00	0.00	0.00	0.00	0.00	0.00	0.00
Math	GSM8K	38.21	0.00	0.00	0.00	0.00	0.00	0.00	0.00	0.00
Gen.	MMLU	62.50	25.24	24.68	25.11	23.43	23.65	24.26	24.26	24.99
	BBH	56.40	0.00	0.00	0.00	0.00	0.00	0.00	0.00	0.01
Avg. Performance Score(↓)		60.59	15.98	16.87	16.55	15.91	16.34	15.84	15.90	17.09
Average Distillation Ratio(↓)		-	26.38	27.85	27.32	26.25	26.97	26.15	26.24	28.20
Average Distillation Ratio(↓)		-	11.50	11.31	11.48	10.71	10.77	11.44	11.02	10.71

Table 31: Evaluation Results of Mistral-7B under Different Secured Layers (Part1)

		16	18	20	22	24	26	28	30	*
Rsn.	PIQA	54.50	52.32	52.72	57.13	62.82	64.67	67.23	75.61	49.35
	Hellaswag	29.31	29.02	29.99	33.46	46.21	52.12	52.46	67.73	25.39
	Winogrande	51.20	54.17	51.07	55.75	58.59	62.41	63.09	66.33	50.59
	ARC_easy	32.84	29.35	30.80	38.04	47.24	51.99	54.74	69.95	25.83
	ARC_challenge	21.19	23.04	23.78	26.34	30.86	33.22	35.04	40.53	22.35
Read.	OpenBookQA	26.00	27.87	26.87	29.67	28.73	32.67	33.40	36.40	25.00
	LAMBADA	2.61	0.18	1.28	4.17	21.89	29.93	24.49	48.32	0.01
	BoolQ	53.98	53.60	58.79	55.76	64.10	74.72	68.48	81.30	45.80
	SQuADv2_em	0.01	0.00	0.47	0.13	2.39	3.59	1.87	1.82	0.00
	SQuADv2_f1	0.96	0.18	1.27	2.60	14.88	22.61	21.12	34.16	0.66
Knl.	NaturalQuestions	0.01	0.10	0.19	0.58	1.84	3.15	3.53	8.87	0.02
	TriviaQA	0.03	0.01	0.61	0.62	5.14	7.51	10.32	25.44	0.01
Code	HumanEval	0.00	0.00	0.00	0.61	2.24	4.88	2.44	9.75	0.00
	MBPP	0.00	0.00	0.00	2.00	4.33	8.33	0.93	13.07	0.00
Math	GSM8K	0.00	0.00	0.00	0.00	0.00	0.00	0.00	0.25	0.00
Gen.	MMLU	24.30	25.84	29.54	24.55	34.77	40.77	40.84	50.44	23.26
	BBH	0.00	0.00	0.02	0.30	7.55	18.76	21.05	30.07	0.00
Avg. Performance Score(↓)		17.47	17.39	18.08	19.51	25.51	30.08	29.47	38.83	15.78
Average Distillation Ratio(↓)		28.83	28.71	29.84	32.20	42.09	49.64	48.64	64.08	26.05
Average Distillation Ratio(↓)		11.34	11.11	10.45	10.59	10.23	10.34	9.59	8.53	11.20

Table 32: Evaluation Results of Mistral-7B under Different Secured Layers (Part2)

		Pretrain	0	2	4	6	8	10	12	14
Rsn.	PIQA	79.27	54.17	72.85	73.76	75.03	76.75	78.00	78.91	77.84
	Hellaswag	73.73	27.61	56.49	57.73	60.47	62.84	66.39	66.91	66.95
	Winogrande	75.45	51.56	59.17	59.98	59.88	64.32	68.11	68.95	70.38
	ARC_easy	79.92	34.57	72.94	73.40	73.97	76.51	78.33	78.66	78.63
	ARC_challenge	52.90	19.45	41.75	39.82	44.11	45.65	47.92	49.74	48.78
Read.	OpenBookQA	51.20	25.80	35.73	37.47	40.13	42.00	44.00	45.67	44.80
	LAMBADA	56.28	3.25	28.55	30.42	34.64	40.05	45.41	45.52	46.66
	BoolQ	83.36	47.29	65.20	62.64	66.39	71.39	73.42	72.95	75.83
	SQuADv2_em	61.30	0.02	10.49	17.63	21.94	33.94	19.54	19.15	29.14
	SQuADv2_f1	71.38	2.61	37.22	40.35	45.53	59.16	48.21	50.09	54.87
Knl.	NaturalQuestions	9.58	0.00	3.60	4.97	6.13	7.55	7.95	8.10	9.25
	TriviaQA	39.29	0.01	13.57	16.29	24.74	28.60	31.58	33.71	32.79
Code	HumanEval	48.78	0.00	1.42	6.50	10.98	16.66	22.76	19.51	23.17
	MBPP	46.80	0.00	5.07	6.87	9.47	19.60	25.67	23.47	25.73
Math	GSM8K	57.77	0.00	7.25	8.64	4.42	9.63	14.18	11.35	17.31
Gen.	MMLU	56.73	26.16	34.29	37.01	39.90	43.11	45.63	48.17	49.82
	BBH	59.53	0.01	15.27	18.37	16.38	14.58	4.93	4.35	11.37
Avg. Performance Score(↓)		59.02	17.21	32.99	34.81	37.30	41.90	42.47	42.66	44.90
Average Distillation Ratio(↓)		-	29.15	55.90	58.99	63.21	71.00	71.97	72.28	76.09
Distillation Difficulty(↑)		-	10.07	7.07	4.95	4.09	3.63	3.31	3.31	3.11

Table 33: Evaluation Results of Phi-2 under Different Secured Layers (Part 1)

		16	18	20	22	24	26	28	30	*
Rsn.	PIQA	77.44	77.80	77.69	76.77	76.89	77.55	78.16	78.58	52.07
	Hellaswag	67.20	66.90	67.13	68.00	68.86	70.01	71.44	71.18	25.26
	Winogrande	70.82	71.40	73.11	74.46	75.79	75.72	75.93	74.77	48.91
	ARC_easy	78.30	77.27	77.33	76.82	78.09	77.76	79.53	79.56	27.03
	ARC_challenge	49.71	48.29	48.52	48.04	49.80	50.68	53.16	52.67	18.66
Read.	OpenBookQA	46.53	46.47	45.87	45.27	46.33	45.53	46.53	48.27	20.80
	LAMBADA	45.67	46.88	47.95	50.17	50.54	52.77	53.01	53.23	0.00
	BoolQ	80.56	80.72	82.22	83.31	83.98	83.54	82.54	83.41	39.60
	SQuADv2_em	7.88	1.30	1.69	1.31	0.15	0.23	3.54	10.03	0.56
	SQuADv2_f1	40.84	34.51	34.25	35.94	35.64	36.68	39.57	44.87	0.90
Knl.	NaturalQuestions	8.90	6.09	6.40	6.79	6.86	6.85	7.20	8.37	0.02
	TriviaQA	31.48	27.03	25.08	24.54	22.89	22.99	24.24	26.93	0.01
Code	HumanEval	22.56	21.34	25.41	32.52	38.01	46.14	46.54	43.90	0.00
	MBPP	26.73	25.33	24.80	31.73	36.67	41.80	43.13	43.20	0.00
Math	GSM8K	16.68	16.02	14.66	12.31	17.24	30.12	45.41	49.79	0.00
Gen.	MMLU	52.69	53.45	55.68	56.61	56.93	56.59	56.86	56.47	22.95
	BBH	3.42	17.36	8.33	18.24	30.09	48.12	52.28	56.36	0.00
Avg. Performance Score(↓)		42.79	42.25	42.12	43.70	45.57	48.42	50.53	51.86	15.10
Average Distillation Ratio(↓)		72.51	71.58	71.38	74.04	77.22	82.04	85.63	87.87	25.59
Distillation Difficulty(↑)		3.07	3.29	3.03	3.01	2.70	2.32	1.98	2.13	11.32

Table 34: Evaluation Results of Phi-2 under Different Secured Layers (Part2). "*" indicates the fully secured model.

		Pretrain	0-1	2-3	4-5	6-7	8-9	10-11	12-13	14-15	16-17	18-19	20-21	22-23	*
Rsn.	PIQA	75.68	53.43	69.52	71.53	73.50	74.76	75.08	74.94	74.64	73.90	74.63	74.54	74.81	50.44
	Hellaswag	62.56	26.27	46.66	50.71	52.98	54.51	55.11	56.01	56.78	57.90	58.76	59.35	58.58	25.05
	Winogrande	72.69	51.09	54.91	59.22	61.75	64.85	67.95	68.88	68.98	71.25	71.19	72.87	70.66	49.12
	ARC_easy	76.14	30.81	61.70	65.70	70.10	71.38	70.01	71.72	71.93	72.34	73.39	74.16	73.74	27.50
	ARC_challenge	44.62	20.56	32.85	34.10	38.08	40.05	40.30	39.48	40.87	41.52	42.84	42.58	45.42	21.22
Read.	OpenBookQA	48.00	26.60	33.93	35.73	40.40	41.13	40.67	41.73	41.67	40.27	41.33	43.27	45.47	26.87
	LAMBADA	44.10	0.59	17.96	26.45	29.37	33.83	33.85	36.46	37.06	37.96	39.98	41.10	40.49	0.00
	BoolQ	75.05	46.98	59.12	52.42	57.41	65.68	68.52	63.47	65.12	66.52	73.91	75.17	77.0	46.28
	SQuADv2_em	48.01	0.00	5.82	10.94	18.34	13.96	14.70	23.22	16.98	26.05	22.04	20.16	26.86	0.00
	SQuADv2_f1	60.84	0.78	24.49	26.04	34.86	32.17	32.36	43.14	38.23	48.03	45.75	45.56	49.62	1.60
Knl.	NaturalQuestions	5.46	0.04	1.68	2.73	3.41	3.06	3.21	4.25	4.03	4.06	4.54	4.17	4.45	0.01
	TriviaQA	16.94	0.01	5.70	7.77	10.85	11.03	9.11	12.11	11.84	11.86	12.02	12.11	13.19	0.01
Code	HumanEval	35.98	0.00	3.05	10.57	12.20	16.26	13.82	17.48	18.70	23.17	29.68	31.91	31.71	0.00
	MBPP	35.40	0.00	2.80	7.80	10.93	17.40	16.53	16.13	16.67	22.27	27.33	28.27	28.53	0.00
Math	GSM8K	30.33	0.00	0.05	0.73	0.15	0.23	0.75	0.50	2.17	4.98	9.73	17.77	23.45	0.00
Gen.	MMLU	42.44	24.07	26.56	28.77	32.51	32.87	36.09	39.42	39.72	43.23	42.51	42.82	43.66	23.95
	BBH	28.80	0.00	2.07	3.97	8.38	7.37	2.81	7.79	4.12	10.63	6.94	10.34	11.45	0.00
Avg. Performance Score(↓)		47.24	16.54	26.40	29.13	32.66	34.15	34.17	36.28	35.85	38.59	39.80	40.95	42.30	15.94
Average Distillation Ratio(↓)		-	35.02	55.90	61.66	69.14	72.29	72.34	76.80	75.90	81.68	84.25	86.69	89.56	33.75
Average Distillation Ratio(↓)		-	10.08	7.18	4.70	3.50	2.93	2.83	2.53	2.36	2.27	2.16	2.06	2.46	9.33

Table 35: Evaluation Results of Phi-1.5 under Different Secured Layers

Llama2-7B		**Phi-2**	
Secure Layers	**GSM8K(↑)**	**Secure Layers**	**GSM8K(↑)**
Fully-open	29.34	**Fully-open**	59.60
0	28.96	**0-1**	59.59
0-4	21.76	**0-5**	58.60
0-8	21.46	**0-9**	58.45
0-12	20.85	**0-13**	55.19
0-16	20.11	**0-17**	56.25
0-20	21.46	**0-21**	54.59
0-24	21.44	**0-25**	55.34
0-28	18.73	**0-29**	54.59
Fully-Secure	20.32	**Fully-Secure**	57.77

Table 36: Customization Performance under Different Secure Sets

		0.25%	0.5%	1%	3%	7%	15%	30%	50%	100%
Rsn.	PIQA	77.78	77.69	67.73	49.42	49.55	50.05	49.98	49.31	49.47
	Hellaswag	71.40	71.54	52.39	25.74	26.03	26.25	25.67	25.48	26.39
	Winogrande	64.64	65.64	54.12	50.38	50.43	49.65	49.59	49.62	50.83
	ARC_easy	74.69	75.04	53.82	26.03	26.76	26.46	26.64	26.66	25.98
	ARC_challenge	43.66	43.29	26.99	20.16	21.39	19.74	21.44	21.73	22.47
Read.	OpenBookQA	63.15	63.62	33.20	0.01	0.00	0.02	0.01	0.01	0.01
	LAMBADA	80.66	80.78	62.10	38.22	39.33	43.45	39.39	41.83	48.34
	BoolQ	11.39	12.14	5.47	0.00	0.00	0.00	0.00	0.00	0.00
	SQuADv2_em	40.24	40.74	32.65	0.78	0.20	0.24	2.09	2.13	0.59
	SQuADv2_f1	40.73	40.67	30.47	22.93	23.40	25.53	24.07	23.07	25.93
Knl.	NaturalQuestions	7.83	7.89	5.61	0.00	0.01	0.02	0.01	0.00	0.04
	TriviaQA	44.29	45.95	18.78	0.00	0.01	0.00	0.00	0.00	0.02
Code	HumanEval	11.39	12.00	0.00	0.00	0.00	0.00	0.00	0.00	0.00
	MBPP	15.20	15.33	1.00	0.00	0.00	0.00	0.00	0.00	0.00
Math	GSM8K	13.22	13.29	0.00	0.00	0.00	0.00	0.00	0.00	0.00
Gen.	MMLU	45.04	45.03	30.90	24.06	24.04	25.01	23.19	23.11	24.45
	BBH	37.45	37.51	17.36	0.00	0.00	0.00	0.00	0.00	0.00
Avg. Performance Score(↓)		43.69	44.01	28.98	15.16	15.36	15.67	15.42	15.47	16.15
Average Distillation Ratio(↓)		84.94	85.56	56.33	29.48	29.86	30.47	29.97	30.07	31.39
Distillation Difficulty(↑)		1.96	1.93	8.66	10.87	11.75	11.48	11.65	11.57	11.19

Table 37: Evaluation Results of Llama2-7B under Different Secure-source Proportion

		20M	50M	100M	160M	200M	300M	600M
Rsn.	PIQA	77.78	73.49	67.55	67.12	49.42	50.36	49.97
	Hellaswag	71.40	63.47	51.67	51.27	25.74	25.70	25.78
	Winogrande	64.64	57.54	53.07	52.04	50.38	49.28	50.49
	ARC_easy	74.69	66.50	51.97	52.11	26.03	26.43	26.29
	ARC_challenge	43.66	36.04	26.51	25.99	20.16	20.79	21.70
Read.	OpenBookQA	63.15	45.34	30.22	28.75	0.01	0.05	0.01
	LAMBADA	80.66	69.47	62.28	62.59	38.22	39.03	40.80
	BoolQ	11.39	2.21	4.18	7.24	0.00	0.00	0.01
	SQuADv2_em	40.24	33.98	28.98	31.05	0.78	0.74	0.37
	SQuADv2_f1	40.73	33.93	29.13	30.00	22.93	23.80	23.53
Knl.	NaturalQuestions	7.83	2.98	5.33	5.73	0.00	0.00	0.02
	TriviaQA	44.29	15.28	13.71	17.25	0.00	0.00	0.01
Code	HumanEval	11.39	0.41	0.00	0.00	0.00	0.00	0.00
	MBPP	15.20	6.87	1.00	0.80	0.00	0.00	0.00
Math	GSM8K	9.00	0.10	0.00	0.00	0.00	0.00	0.00
Gen.	MMLU	45.04	36.15	28.95	29.04	24.06	23.70	23.45
	BBH	37.45	28.53	14.99	16.99	0.00	0.00	0.00
Avg. Performance Score(↓)		43.44	33.66	27.62	28.12	15.16	15.29	15.44
Average Distillation Ratio(↓)		84.46	65.44	53.69	54.66	29.48	29.72	30.01
Distillation Difficulty(↑)		1.96	5.48	8.95	9.25	10.87	10.93	10.81

Table 38: Evaluation Results of Llama2-7B under Different Secure-source Quantity

		0.25%	1%	0.5%	3%	7%	15%	30%	50%	100%
Rsn.	PIQA	77.79	74.36	52.16	53.34	52.07	52.19	50.04	50.60	49.35
	Hellaswag	71.31	65.50	26.50	26.16	25.92	25.91	25.87	25.61	25.39
	Winogrande	67.09	60.32	49.22	51.65	50.01	51.36	51.36	49.65	50.59
	ARC_easy	74.52	69.51	29.95	30.82	29.73	30.44	28.20	27.45	25.83
	ARC_challenge	42.32	38.40	20.76	20.71	21.10	20.25	22.61	22.47	22.35
Read.	OpenBookQA	42.13	34.60	25.13	25.33	26.47	26.07	25.20	25.87	25.00
	LAMBADA	55.99	44.36	0.73	1.66	0.96	0.31	0.03	0.02	0.01
	BoolQ	78.35	74.06	43.18	42.01	42.09	40.02	38.53	39.91	45.80
	SQuADv2_em	13.91	6.97	0.00	0.01	0.00	0.00	0.00	0.00	0.00
	SQuADv2_f1	41.13	33.88	1.60	0.93	1.27	0.71	0.99	0.86	0.66
Knl.	NaturalQuestions	8.46	5.82	0.03	0.00	0.02	0.03	0.00	0.00	0.02
	TriviaQA	34.04	17.03	0.01	0.01	0.02	0.01	0.00	0.00	0.01
Code	HumanEval	11.99	6.51	0.00	0.00	0.00	0.00	0.00	0.00	0.00
	MBPP	16.93	12.80	0.00	0.00	0.00	0.00	0.00	0.00	0.00
Math	GSM8K	6.32	0.45	0.00	0.00	0.00	0.00	0.00	0.00	0.00
Gen.	MMLU	44.17	37.98	23.98	24.34	25.10	23.91	23.68	24.12	23.26
	BBH	35.44	27.27	0.02	0.00	0.00	0.00	0.00	0.00	0.00
Avg. Performance Score(↓)		42.46	35.87	16.08	16.29	16.16	15.95	15.68	15.68	15.78
Average Distillation Ratio(↓)		70.08	59.20	26.53	26.89	26.67	26.33	25.87	25.88	26.05
Distillation Difficulty(↑)		2.22	5.48	10.92	11.29	11.35	11.19	11.17	11.20	11.20

Table 39: Evaluation Results of Mistral-7B under Different Secured Proportion

		20M	50M	100M	160M	200M	300M	600M
Rsn.	PIQA	77.79	73.74	51.36	52.86	53.34	50.98	51.62
	Hellaswag	71.31	65.51	26.49	27.98	26.16	26.27	26.04
	Winogrande	67.09	64.51	50.06	49.51	51.65	50.17	50.85
	ARC_easy	74.52	68.29	27.84	30.95	30.82	27.36	28.30
	ARC_challenge	42.32	37.97	20.85	21.67	20.71	21.28	20.17
Read.	OpenBookQA	42.13	37.27	25.60	25.87	25.33	26.60	27.00
	LAMBADA	55.99	47.63	1.16	4.74	1.66	0.43	0.53
	BoolQ	78.35	75.00	40.17	47.05	42.01	42.05	39.03
	SQuADv2_em	13.91	8.65	0.01	0.04	0.01	0.01	0.00
	SQuADv2_f1	41.13	35.50	1.01	0.49	0.93	0.28	0.39
Knl.	NaturalQuestions	8.46	7.82	0.02	0.05	0.00	0.01	0.02
	TriviaQA	34.04	22.89	0.02	0.19	0.01	0.01	0.01
Code	HumanEval	11.99	7.93	0.00	0.00	0.00	0.00	0.00
	MBPP	16.93	11.87	0.00	0.00	0.00	0.00	0.00
Math	GSM8K	6.32	2.48	0.00	0.00	0.00	0.00	0.00
Gen.	MMLU	44.17	41.28	24.22	24.44	24.34	23.78	23.33
	BBH	35.44	33.43	0.00	0.40	0.00	0.00	0.00
Avg. Performance Score(↓)		42.46	37.75	15.81	16.84	16.29	15.84	15.72
Average Distillation Ratio(↓)		70.08	62.31	26.10	27.79	26.89	26.14	25.95
Distillation Difficulty(↑)		2.22	3.44	11.14	10.85	11.10	11.23	11.22

Table 40: Evaluation Results of Mistral-7B under Different Secured Quantity

		0.25%	0.5%	1%	3%	7%	15%	30%	50%	100%
Rsn.	PIQA	70.40	70.71	74.64	54.43	54.17	54.75	54.37	52.39	52.07
	Hellaswag	53.13	52.99	62.84	27.88	27.61	27.77	28.01	26.30	25.26
	Winogrande	66.17	66.43	69.93	51.49	51.56	51.46	51.44	49.12	48.91
	ARC_easy	64.62	65.33	72.55	33.39	34.57	32.00	32.18	29.97	27.03
	ARC_challenge	43.26	43.86	40.67	20.82	19.45	20.00	20.56	19.88	18.66
Read.	OpenBookQA	41.80	42.67	38.87	26.87	25.80	26.33	26.53	26.07	20.80
	LAMBADA	32.51	32.25	40.24	10.58	3.25	3.87	6.06	0.66	0.00
	BoolQ	65.77	65.27	76.84	48.13	47.29	45.62	46.15	40.50	39.60
	SQuADv2_em	0.36	9.09	3.31	0.02	0.02	0.01	0.01	0.00	0.56
	SQuADv2_f1	24.81	30.83	30.47	0.45	2.61	0.57	2.52	1.67	0.90
Knl.	NaturalQuestions	5.70	5.06	1.14	0.03	0.00	0.01	0.07	0.03	0.02
	TriviaQA	20.27	21.50	8.78	2.02	0.01	0.02	0.01	0.01	0.01
Code	HumanEval	22.16	26.83	17.68	0.00	0.00	0.00	0.00	0.00	0.00
	MBPP	25.07	26.40	9.73	0.00	0.00	0.00	0.00	0.00	0.00
Math	GSM8K	29.26	31.36	2.00	0.00	0.00	0.00	0.00	0.00	0.00
Gen.	MMLU	41.76	42.17	43.86	30.31	26.16	25.79	24.85	24.03	22.95
	BBH	18.98	21.55	9.59	3.06	0.01	0.79	0.24	0.00	0.00
Avg. Performance Score(↓)		36.83	38.49	35.48	18.20	17.21	17.00	17.24	15.92	15.10
Average Distillation Ratio(↓)		62.40	65.22	60.12	30.95	29.15	28.81	29.21	26.97	25.59
Distillation Difficulty(↑)		6.70	6.65	2.00	9.14	10.07	10.13	10.14	9.82	11.32

Table 41: Evaluation Results of Phi-2 under Different Secured Proportion

		20M	50M	100M	160M	200M	300M	600M
Rsn.	PIQA	73.70	70.00	53.90	54.17	53.01	54.75	54.28
	Hellaswag	59.75	55.64	28.26	27.61	26.90	27.77	28.61
	Winogrande	66.61	67.17	51.96	51.56	52.28	51.46	50.88
	ARC_easy	70.96	67.02	35.17	34.57	31.84	32.00	31.62
	ARC_challenge	48.30	42.52	21.84	19.45	20.39	20.00	20.56
Read.	OpenBookQA	45.33	41.27	26.13	25.80	25.60	26.33	26.53
	LAMBADA	35.64	25.34	1.93	3.25	2.17	3.87	5.78
	BoolQ	75.37	66.25	51.66	47.29	40.81	45.62	47.69
	SQuADv2_em	10.62	0.10	0.14	0.02	0.02	0.01	0.00
	SQuADv2_f1	38.28	22.83	1.33	2.61	1.36	0.57	1.13
Knl.	NaturalQuestions	5.44	4.51	0.06	0.00	0.02	0.01	0.05
	TriviaQA	12.34	12.77	0.05	0.01	0.01	0.02	0.01
Code	HumanEval	20.94	10.98	0.00	0.00	0.00	0.00	0.00
	MBPP	12.60	13.40	0.00	0.00	0.00	0.00	0.00
Math	GSM8K	7.52	7.78	0.00	0.00	0.00	0.00	0.00
Gen.	MMLU	43.07	39.45	26.26	26.16	25.85	25.79	25.38
	BBH	12.35	18.02	0.00	0.01	0.00	0.79	0.12
Avg. Performance Score(↓)		37.57	33.24	17.57	17.21	16.49	17.00	17.22
Average Distillation Ratio(↓)		63.67	56.32	29.77	29.15	27.93	28.81	29.17
Distillation Difficulty(↑)		2.07	7.96	9.25	9.96	10.08	10.13	10.22

Table 42: Evaluation Results of Phi-2 under Different Secured Quantity

		0.25%	0.5%	1%	3%	7%	15%	30%	50%	100%
Rsn.	PIQA	68.21	68.37	69.68	65.85	53.43	52.94	52.36	51.25	50.44
	Hellaswag	49.05	49.18	49.30	30.72	26.27	26.74	27.02	26.10	25.05
	Winogrande	63.83	64.91	61.20	58.04	51.09	51.38	50.25	50.22	49.12
	ARC_easy	62.94	62.89	62.25	35.15	30.81	29.27	29.64	27.99	27.50
	ARC_challenge	36.98	37.49	32.91	25.97	20.56	20.36	20.08	20.88	21.22
Read.	OpenBookQA	39.07	40.20	35.00	33.87	26.60	27.67	27.73	26.47	26.87
	LAMBADA	24.71	24.99	25.36	0.11	0.59	0.78	1.15	0.06	0.00
	BoolQ	59.43	59.35	63.49	41.01	46.98	51.59	46.46	44.02	46.28
	SQuADv2_em	15.65	16.00	3.13	0.50	0.00	0.01	0.03	0.00	0.00
	SQuADv2_f1	32.62	32.62	14.88	0.56	0.78	1.24	2.29	1.58	1.60
Knl.	NaturalQuestions	2.72	2.64	0.32	0.03	0.04	0.03	0.05	0.03	0.01
	TriviaQA	8.17	7.96	5.69	0.01	0.01	0.01	0.01	0.01	0.01
Code	HumanEval	14.43	13.41	2.03	0.00	0.00	0.00	0.00	0.00	0.00
	MBPP	17.20	18.67	6.47	0.00	0.00	0.00	0.00	0.00	0.00
Math	GSM8K	4.88	4.90	0.25	0.00	0.00	0.00	0.00	0.00	0.00
Gen.	MMLU	30.12	29.88	28.98	27.78	24.07	24.22	24.66	24.28	22.95
	BBH	4.34	3.19	0.98	0.50	0.00	0.00	0.00	0.00	0.00
Avg. Performance Score(↓)		31.43	31.57	27.17	19.41	16.54	16.84	16.57	16.05	15.94
Average Distillation Ratio(↓)		66.54	66.83	57.52	41.11	35.02	35.64	35.08	33.98	33.75
Distillation Difficulty(↑)		6.18	6.15	2.76	9.28	10.08	11.19	10.54	10.23	11.26

Table 43: Evaluation Results of Phi-1.5 under Different Secured Proportion

		20M	50M	100M	160M	200M	300M	600M
Rsn.	PIQA	69.80	65.85	53.43	52.52	52.94	53.06	53.81
	Hellaswag	49.51	25.72	30.27	26.31	26.74	27.05	26.51
	Winogrande	62.56	58.04	51.09	50.83	51.38	50.57	49.99
	ARC_easy	62.41	30.15	30.81	29.14	29.27	29.62	29.67
	ARC_challenge	32.51	25.97	20.56	19.97	20.36	20.48	20.79
Read.	OpenBookQA	35.53	33.87	26.60	26.93	27.67	28.20	26.87
	LAMBADA	28.14	0.11	0.59	0.45	0.78	1.30	0.61
	BoolQ	64.77	41.01	46.98	47.33	51.59	46.09	45.59
	SQuADv2_em	4.67	0.50	0.00	0.00	0.01	0.01	0.00
	SQuADv2_f1	22.47	0.56	0.78	1.02	1.24	2.31	2.01
Knl.	NaturalQuestions	1.64	0.03	0.04	0.05	0.03	0.06	0.03
	TriviaQA	5.93	0.01	0.01	0.01	0.01	0.02	0.01
Code	HumanEval	7.73	0.00	0.00	0.00	0.00	0.00	0.00
	MBPP	7.87	0.00	0.00	0.00	0.00	0.00	0.00
Math	GSM8K	0.28	0.00	0.00	0.00	0.00	0.00	0.00
Gen.	MMLU	31.11	27.78	24.07	23.41	24.22	24.54	24.68
	BBH	3.38	0.50	0.00	0.00	0.00	0.00	0.00
Avg. Performance Score(↓)		28.84	19.89	16.54	16.35	16.84	16.67	16.50
Average Distillation Ratio(↓)		61.06	41.11	35.02	34.61	35.64	35.28	34.94
Distillation Difficulty(↑)		2.81	9.28	10.26	11.65	11.19	10.87	10.49

Table 44: Evaluation Results of Phi-1.5 under Different Secured Quantity

		Pretrain	0-2	3-5	6-8	9-11	12-14	15-17	18-20	21-23	24-26	27-29	30-32	33-35	*
Rsn.	PIQA	64.69	61.40	62.50	61.11	56.46	58.47	58.94	61.86	62.59	63.13	61.93	62.67	63.11	49.53
	Hellaswag	36.68	34.03	34.27	33.69	31.79	32.24	32.78	33.27	33.68	33.25	33.94	33.63	33.07	25.77
	Winogrande	52.09	51.62	52.96	51.57	50.83	52.83	51.06	51.52	51.85	52.06	52.04	51.99	50.94	49.85
	ARC_easy	44.02	40.46	40.66	40.07	35.41	37.50	37.81	39.91	40.70	41.12	41.19	40.84	39.92	26.53
	ARC_challenge	20.82	22.27	22.61	21.25	21.39	21.25	22.01	21.36	20.25	20.48	19.88	20.99	20.28	19.82
Read.	OpenBookQA	28.00	27.60	27.47	27.40	27.40	27.27	26.20	26.47	27.67	26.80	28.67	27.67	27.13	27.47
	LAMBADA	40.47	30.62	32.97	28.62	21.65	23.87	28.23	29.07	29.83	29.81	31.72	31.43	18.08	0.00
	BoolQ	57.74	50.87	48.51	50.58	51.60	52.83	53.42	54.37	53.30	51.42	59.79	53.14	60.42	37.83
	SQuADv2_em	11.34	6.87	7.88	4.74	4.19	0.27	0.87	2.22	3.79	3.05	4.11	4.69	2.35	0.00
	SQuADv2_f1	19.35	16.27	17.00	12.00	11.72	9.04	6.92	10.11	10.90	10.08	8.88	11.47	7.30	0.01
Knl.	NaturalQuestions	1.08	1.05	0.83	0.83	0.78	0.55	0.69	0.41	1.00	0.85	0.71	0.52	0.75	0.04
	TriviaQA	4.48	2.24	2.66	2.01	2.16	1.41	1.06	2.39	2.38	2.29	1.57	1.90	1.76	0.02
Code	HumanEval	0.00	0.00	0.00	0.00	0.00	0.00	0.00	0.00	0.00	0.00	0.00	0.00	0.00	0.00
	MBPP	0.00	0.00	0.00	0.00	0.00	0.00	0.00	0.00	0.00	0.00	0.00	0.00	0.00	0.00
Math	GSM8K	1.59	0.15	0.25	0.00	0.08	0.00	0.05	0.00	0.03	0.18	0.00	0.00	0.00	0.00
Gen.	MMLU	26.05	25.52	26.02	25.20	25.60	25.05	25.73	23.97	25.57	26.04	25.13	25.17	25.73	22.95
	BBH	16.97	6.87	12.58	5.51	5.11	2.55	5.98	2.74	11.15	13.98	14.25	13.02	12.57	0.00
Avg. Performance Score(↓)		25.02	22.23	22.89	21.44	20.36	20.30	20.69	21.16	22.04	22.03	22.58	22.30	21.38	15.28
Average Distillation Ratio(↓)		-	88.83	91.49	85.71	81.38	81.13	82.69	84.55	88.08	88.05	90.23	89.13	85.43	61.08
Distillation Difficulty(↑)		-	5.92	9.32	9.04	8.60	8.83	8.73	7.17	5.82	5.18	4.65	4.92	4.15	10.89

Table 45: Evaluation Results of OPT-350M under Different Secured Layers. "*" indicates the fully secured model.